ChemSusChem

Supporting Information

Chemo-Biological Upcycling of Poly(ethylene terephthalate) to Multifunctional Coating Materials

Hee Taek Kim[+], Mi Hee Ryu[+], Ye Jean Jung, Sooyoung Lim, Hye Min Song, Jeyoung Park, Sung Yeon Hwang, Hoe-Suk Lee, Young Joo Yeon, Bong Hyun Sung, Uwe T. Bornscheuer, Si Jae Park,* Jeong Chan Joo,* and Dongyeop X. Oh*This publication is part of a collection of invited contributions focusing on " Chemical Upcycling of Waste Plastics". Please visit to view all contributions.

Table of Contents

Definitions of Terms

BHET: (Bis(2-hydroxyethyl) terephthalic acid, MW: 254 g/mol): BHET is an organic molecule that consists of two ethylene glycols (EG) and one terephthalic acid (TPA) wherein two EGs are bonded at both ends of TPA by ester bonds. BHET is the target product of conventional glycolysis of PET.
***g*-BHET:** In this study, BHET obtained by glycolysis of PET waste has been named *g*-BHET.
MHET: (Mono-(2-hydroxyethyl) terephthalic acid, MW : 210 g/mol): MHET is an organic molecule that consists of one EG and one TPA linked each other by an ester bond. MHET can be formed by the partial hydrolysis of BHET during glycolysis or enzymatic hydrolysis. In enzymatic hydrolysis, BHET can be rapidly hydrolyzed to MHET and EG by esterase Bs2Est.
TPA: (Terephthalic acid, MW: 166 g/mol): TPA, Benzene-1,4-dicarboxylic acid, is the final target product of the chemo-enzymatic depolymerization. In this study, TPA is used as a substrate to biosynthesize catechol by an engineered microorganism.
PET oligomers: PET oligomers, insoluble fractions, are formed by incomplete depolymerization of PET. PET oligomers are detected mainly as a dimer and a small proportion of trimer and tetramer. In this study, one of the main topics is to develop the enzymatic hydrolysis of PET oligomers and to elucidate how Bs2Est is able to hydrolyze the dimer.
Dimer: (EG-(TPA-EG)$_2$, MW: 446 g/mol): In this study, a substance (EG-TPA-EG-TPA-EG) wherein two TPAs are linked by ester bonds to three EGs is defined as a dimer because ester bonds in PET are depolymerized by the addition of EG. The dimer is an insoluble fraction in the glycolysis formed by incomplete depolymerization of PET at the low temperature or due to short reaction times.
TPA-EG-TPA(-EG): TPA-EG-TPA(-EG) are potential hydrolysis products by an exo-cleavage activity of esterase toward dimer (EG-TPA-EG-TPA-EG). The molecular weights of TPA-EG-TPA and TPA-EG-TPA-EG are 358 and 402 g/mol, respectively. The formation of these compounds during the enzymatic hydrolysis of the glycolyzed products means that esterase hydrolyzes PET oligomers by an exo-cleavage activity.
Trimer: (EG-(TPA-EG)$_3$, MW: 639 g/mol) **and tetramer** (EG-(TPA-EG)$_4$, MW : 831 g/mol): Trimer and tetramer, like the dimer, are the oligomeric compounds formed by incomplete depolymerization of PET after glycolysis.

Experimental Procedures

Materials.

Disposable PET bottles were obtained from Appendix (Korean local coffee chain), Starbucks, and McDonald's. PET pieces were obtained by cutting waste plastic coffee cups into 3x3 mm^2 and used for glycolysis after the validation by comparing their functional groups and purity with those of reagent-grade PET (Fig. S1). K_2CO_3 (99.5%), hydrochloric acid (35-37%), and glycerol (99%) were purchased from SAMCHUN Inc (Seoul, Korea). Ethylene glycol (≥ 99%), bis(2-hydroxyethyl) terephthalate (BHET, 98%), terephthalic acid(TPA), potassium phosphate dibasic (≥ 98%), catechol (≥ 99%), 0.1 wt% poly-L-lysine aqueous solution, chitosan powder (141 kDa), trifluoroacetic acid and silver nitrate ($AgNO_3$; HPLC grade) were acquired from Sigma-Aldrich (St. Louis, USA). Tris-HCl buffer (1 M, pH 8.5) and potassium dihydrogen phosphate (> 98%) were purchased from iNtRON Biotechnology (Seongnam, Korea) and Duchefa Biochemie (Haarlem, Netherlands) respectively. Mono-(2-hydroxyethyl) terephthalic acid (MHET, 97%) was obtained from Advanced ChemBlocks Inc (Burlingame, USA). Methanol (HPLC grade) was supplied from DUKSAN Inc (Ansan, Korea). Water (≥ 99.9%, J.T. Baker, Delaware County, USA), acetonitrile (≥ 99.9%, J.T. Baker), chloroform (≥ 99.9%, J.T. Baker), and formic acid (85%, SKC, Seongnam, Korea) were used as mobile phases. PET film with a thickness of 50 μm was kindly provided by SKC (Seoul, Korea). Chitosan (0.1 wt%) was prepared by dissolving 1 g of chitosan powder into 1 L of acetic acid aqueous solution (0.1%). 3.25 mM $AgNO_3$ aqueous solution was prepared by dissolving silver nitrate in acetate buffer (pH 4).

Analysis

For NMR analysis of substrates and glycolyzed products, the chemicals were dissolved in d_6-DMSO, D_2O or *d*-trifluoroacetic acid according to the properties of chemicals. All experiments were performed and recorded on a model of Bruker AVANCE ^{1}H-NMR 500 MHz and ^{13}C-NMR 125 MHz. FT-IR spectroscopy analysis was carried out using a Bruker ALPHA-P&ALPHA-T spectrometer equipped with a DTGS detector to characterize the chemical structures of PET, PET oligomers, BHET, and EG. All measurements of samples were performed with attenuated total reflectance (ATR) mode, 256 scans, in the frequency range of 4000-400 cm^{-1}. Thermal analysis of all PET samples was measured by differential scanning calorimetry (DSC) with a Q1000 (TA Instrument, New Castle, US). 1–3 mg of film sample were heated at a rate of 10 °C/min from room temperature to 280 °C in an N_2 atmosphere. Gel permeation

chromatography (GPC) equipped with Plgel Mixed-C and Plgel Mixed-D (Agilent, USA) was used to analyze the weight distribution of the PET oligomers. BHET, MHET, and TPA were analyzed by high-performance liquid chromatography (HPLC) with ZORBAX Eclipse Plus C18 (5 μm, Agilent). The temperature of the column was 35 °C and the flow rate was 0.8 mL/min. The mobile phase was changed gradually from 95% deionized water containing 0.1% (v/v) of formic acid to 30% acetonitrile at 20 min. The UV detector operated at 260 nm. The mass of the PET oligomers was analyzed on Bruker Autoflex Speed TOF/TOF Matrix-Assisted Laser Desorption Ionization-Time of Flight-Mass Spectrometer (MALDI-TOF-MS). The samples were dissolved in DMSO as a solvent and 2,5-dihydroxybenzoic acid (DHB) as a matrix. Chloroform was used as the eluent with a flow rate of 1 mL/min and the column temperature was 40 °C. The sample was monitored by Refractive Index (RI) detector (Viscotek VE 3580). The OD_{600} of *Escherichia coli* (*E. coli*) cells was measured using a spectrophotometer (UV-1700, Shimadzu). Concentrations of TPA and catechol were determined by an HPLC equipped with Optimapak C18 column (RStech, Daejeon, Korea). The column temperature was maintained at 30 °C and the mobile phase consisted of 10% (v/v) acetonitrile in 0.1% (v/v) trifluoroacetic acid in deionized water at a 1.0 mL/min flow rate. The injection volume was 5 μL, and UV detection was performed at 254 and 270 nm. The contact angle was measured using an SEO 300A (Surface and Electro‐Optics Co., Korea). The drop volume used for the measurement is 5 μL and macroscopic images of the droplet were taken by a camera. The antibacterial activity was evaluated by Kirby-Bauer method for gram-negative (*E. coli* ATCC 25922) bacteria. The pristine film was used as a negative control. The sample films were placed on Lysogenic broth (LB) agar plates containing bacterial cells in log-phase and incubated overnight at 37 °C. The area of the inhibition zone was measured in triplicate using an image analysis software: ImageJ v.148 (National Institutes of Health, Bethesda, MD, USA). For the cell adsorption test, a fibroblast cell line L-929 was seeded on the coated-films in 24-well plates with 10^4 cells per well and cultured to adhere at 36 ± 1 °C for 24 h in 5% CO_2 atmosphere in Dulbecco's modified Eagle's medium (DMEM) supplemented with 10% FBS, 100 U/mL penicillin G, 100 μg/mL streptomycin, and 0.025 μg/mL amphotericin B. To evaluate the viability, the media was replaced by 300 μl of 10% (Cell Counting Kit-8, CK04, Dojindo, Inc., Rockville, MD, USA) (CCK-8) solution which can measure cellular respiration activity. Afterward, L929 cells were incubated for 2 h at 36 ± 1 °C. The incubated media were transferred to fresh 96-well plates for the colorimetric assessment using a microplate reader at 450 nm. The data of quintuplicate samples are expressed as mean ± the standard deviation.

Selection of esterase used for the development of chemo-enzymatic depolymerization

To find candidate enzymes suitable for the chemo-enzymatic depolymerization, four commercially available esterases, esterase from *Bacillus subtilis* (cat. #96667), *Paenibacillus barcinonensis* (cat. #04492), *Rhizopus oryzae* (cat. #79208), and *Methylobacterium populi*, (cat. #80712) were tested. All esterases were purchased from Sigma-Aldrich. The esterase activity of four candidate enzymes was measured using *p*-nitrophenyl acetate (*p*NPA) as a model substrate.[1] To examine the BHET-hydrolytic activity of four esterases, 1 U/mL of enzymes was added to the reaction mixture containing 4 mM of BHET in 50 mM Tris-HCl buffer (pH 7.5) and then reacted at 30 ºC for 24 h. The resultant products were analyzed using the HPLC system.

Plasmids construction and transformation

E. coli XL1-Blue (Stratagene, San Diego, CA) was used as a host strain for plasmid construction and whole-cell biotransformation. *E. coli* BL21 (DE3) was used as a host strain for protein expression. DNA cloning was performed according to standard procedures.[2] PCR was performed using a C1000 Thermal Cycler (Bio-Rad, Hercules, CA). The genes and the primers used in this study are listed in Table S2 and Table S3, respectively. For the construction of pET28a-Bs2Est used for enzymatic hydrolysis, pET28a and the synthetic gene of Bs2Est [3] were digested by *Xho*I and *Nde*I and then ligated each other. pET28a-Bs2Est plasmid was transformed into *E. coli* BL21 (DE3) for heterologous expression of the Bs2Est enzyme. For the construction of pKE112TphBaroY and pKM212TphAabc, pKE112 and pKM212 were digested first by *Ecor*I/*Kpn*I and *Kpn*I/*Hind*III, respectively. The *tphAabc* and *tphB* genes were also digested by *Ecor*I/*Kpn*I and *Kpn*I/*Hind*III and then ligated into pKE112 and pKM212, respectively. Finally, the pKE112TphBAroY plasmid was constructed by ligating of *aroY* gene digested by *BamH*I/*Sbf*I into the same digested sites of pKE112TphB. After DNA sequencing of pKE112TphBaroY and pKM212TphAabc plasmids, they were transformed into *E. coli* XL1-Blue to construct a biosynthetic strain-producing catechol from TPA. The recombinant strains were grown in LB media (10 g/L tryptone, 10 g/L NaCl, and 5 g/L yeast extract) or on LB agar plate (agar 2 % w/v) with proper antibiotics (50 μg/mL of ampicillin and 40 μg/mL of kanamycin). All strains and plasmids used in this study were listed in Table S4.

Preparation of purified recombinant Bs2Est

Bs2Est enzyme was produced using *E. coli* BS2 strain as follows (Table S4). For seed cultures, *E. coli* BS2 strain was cultivated overnight at 37 °C 200 rpm in 10 mL LB media supplemented with proper antibiotics. The 5 mL of seed cultures were incubated in 250 mL of LB media and incubated at 37 °C and 200 rpm until the culture optical density (OD 600 nm) reached 0.4-0.6. Then, Bs2Est expression was induced with 0.1 mM IPTG. After induction, cells were further cultivated at 20 °C and 180 rpm for 24 h. *E. coli* cells were harvested by centrifugation at 11600×*g* for 10 min at 4 °C, and then washed twice with proper buffer (pH 7.5). The washed cells were resuspended in 50 mM potassium phosphate buffer (pH 8.0) containing 1X Protease Inhibitor Mini Tablets (Pierce, Thermo Scientific) and 1 mg/mL lysozyme and disrupted by sonication (10-sec pulse on, 15-sec pulse off, AMP 20%). The disrupted cells were centrifuged at 4 °C and 11600×*g* for 1 h and then the supernatants were filtrated by 0.22 μm filter (Choice filter, Thermo Scientific). The supernatant was incubated with a Ni-affinity resin (Qiagen, Valencia, USA) for 1 h and was washed 5 times with the same volume of washing buffer (50 mM sodium phosphate buffer, 300 mM sodium chloride, and 20 mM imidazole, pH 8.0). Then, the affinity resin was eluted with elution buffer (50 mM sodium phosphate buffer, 300 mM sodium chloride, and 250 mM imidazole, pH 8.0). Purified Bs2Est was concentrated using 30 kDa Amicon Ultra centrifuge tube (Millipore, Burlington, USA). Before the enzyme reaction, the concentration and esterase activity of Bs2Est were quantified by Bradford and *p*NPA assays, respectively. The enzyme concentration of Bs2Est (2 U/mL) used in enzymatic hydrolysis was 41.8 μg/mL.

Bs2Est activity assay by *p*NPA and kinetic values

The esterase activity of purified Bs2Est was determined using the *p*NPA assay. Purified Bs2Est was diluted to 0.1 mg/mL and 20 µL of diluted enzyme solution was added to 230 µL assay buffer (10 µL of 50 mM of pNPA dissolved in acetonitrile, 40 µL ethanol and 950 µL of 50 mM sodium phosphate buffer in 1 mL assay buffer, pH 7.5). Then, the change of absorbance was monitored at 405 nm and 30 °C using a multiplate scanner (Multiskan GO, Thermo Scientific). One enzyme unit of Bs2Est (1 U) was defined as the amount of enzyme which converts 1 µmol *p*-nitrophenylacetate per minute at pH 7.5 and 30 °C. For determination of kinetic parameters (K_M, V_{max}, k_{cat}, and k_{cat}/K_M) toward BHET or MHET, enzyme reactions were performed in 50 mM sodium phosphate buffer (pH 7.5) at 30 °C with different concentrations of substrates, 0.5–20 mM of BHET or 0.5–14 mM of MHET, respectively. The kinetic parameters were determined by Lineweaver–Burk plot method.

Theoretical maximum hydrolysis yield

The theoretical maximum hydrolysis yield is calculated by dividing actual molar concentration TPA formed by chemo-enzymatic depolymerization reaction of PET by the theoretical maximum concentration of TPA produced from PET pieces [Eq. S1]. The theoretical maximum concentration of TPA is determined by dividing the initial weight of PET samples by the molecular weight of the repeating unit (TPA-EG).

$$\text{Theoretical maximum hydrolysis yield } ([\text{mol/mol}]\%) = \frac{Actual\ molar\ concentration\ of\ TPA\ (m)}{\frac{Concentration\ of\ PET\ (g/l)}{Molecular\ weight\ of\ PET\ repeating\ unit\ (g/mol)}} \times 100 \quad \textbf{[Eq. S1]}$$

Effect of pH on Bs2Est

The effect of pH on the TPA conversion was investigated in 50 mM sodium phosphate buffer containing 2 mM of MHET and 2 U/mL of Bs2Est at 30 °C and different pH values (pH 6-8). The production of TPA was analyzed by the HPLC system with the ZORBAX Eclipse Plus C18 system. The concentrations of TPA produced at different pH values were compared with that obtained at the control pH 7.5.

Inhibitory effect of EG, TPA disodium salt on Bs2Est

To examine the product inhibition of Bs2Est by EG or TPA, enzyme reactions were performed in the concentration range of EG (0-40 mM) or TPA disodium salt (0-16 mM). In the presence of EG or TPA, 2 mM of BHET was hydrolyzed using 2 U/mL of Bs2Est in 50 mM sodium phosphate buffer (pH 7.5) at 30 °C. For pH titration, a Metrohm 906 Titrando (Herisau, Switzerland) was used to adjust pH 7.5 in enzyme reactions by adding the proper amount of 1 N NaOH.

Residual activity of Bs2Est after enzymatic reactions

In order to measure the residual enzyme activity, Bs2Est was harvested after the termination of the enzyme reaction (8 h) with 4 mM or 24 mM of BHET in 50 mM sodium phosphate buffer (pH 7.5) containing 2 U/mL of Bs2Est, wherein initial enzyme loading was 0.32 mg/mL. To recover pure Bs2Est from reaction mixtures, the harvested enzyme solution was repeatedly exchanged with a fresh buffer and concentrated using 30-kDa sized Amicon Ultra centrifuge tube. Then, the initial enzyme rate was measured to measure the residual activity after quantifications of the enzyme concentration and esterase activity by Bradford assay and *p*NPA assay, respectively. The enzyme reaction was performed in 50 mM sodium phosphate buffer (pH 7.5) containing 2 mM of MHET and 0.5 U/mL of Bs2Est at 30°C. To examine the potential inhibitory action by the acid form of TPA, the enzyme solution was pre-incubated with 3 mM or 6 mM TPA acid in 50 mM Tris-HCl buffer (pH 7.5) for 8 h and then the residual activity was measured. All experiments were conducted in triplicate, and the enzyme reaction mixtures were analyzed using HPLC.

Solubility test of TPA and variation of pH

To test the solubility of TPA in 50 mM Tris-HCl buffer and 50 mM sodium phosphate buffer, a proper amount of TPA was added to 50 mM Tris-HCl buffer to make an initial concentration of TPA from 1 to 10 mM. In the same manner, TPA was added to 50 mM sodium phosphate buffer to prepare the solution of TPA in a concentration of 0.6 to 30 mM. The solution of TPA was stirred for 3 h at room temperature. Then, pH values and concentration of the TPA solutions were measured using pH meter and HPLC system with ZORBAX Eclipse Plus C18 as described above.

***In silico* modeling of Bs2Est**

Each step of molecular modeling was carried out using the Maestro modeling package version 11.8.012 (Schrödinger, Inc., New York, NY, USA) implementing OPLS3e force field. The homology model of Bs2Est was generated based on the crystal structure of *p*-nitrobenzyl esterase (PDB ID: 1QE3), in which two missing loops were added from the organophilic mutant 5-6c8 (PDB ID: 1C7J). [4] The sequence identities of the two templates to the Bs2Est were 97.75% and 96.32%, respectively. The enzyme structure was optimized by Protein Preparation Wizard in Maestro with the addition of missing hydrogens, H-bond assignment, and restrained minimization. Ligands were generated separately and optimized via LigPrep. A receptor grid in Bs2Est for docking of the ligands was defined by a 20 x 20 x 20 Å box to encompass the catalytic triad, S189, H399, and E310, and the oxyanion stabilizing loop G105-F108. [5] The docking of the ligands in the box was carried out by Standard Precision mode of Glide.[6] For the molecular dynamics simulation via Desmond, the TIP3P solvent model surrounding the Bs2Est, with the S189 covalently bound to the tetrahedral intermediates of the docked ligands, was subjected to 10 ns simulation with conditions such as an NVT ensemble, 303 K, and a time step of 1 ps.

Additional Results and Discussion

Analysis of PET pieces

In this study, the waste plastic coffee cup was used for PET glycolysis. NMR and FT-IR analyses were performed to confirm that PET piece from the waste plastic coffee cup was the identical component with reagent-grade PET before performing the glycolysis. It was revealed that H_a and H_b, which are characteristic peaks present in NMR spectra of PET, were the same and that other impurities were not present. The absence of a peak around 3400 cm^{-1} appeared by the hydroxyl group indicates indirectly that it is high molecular weight PET in IR spectra. It was found that these two materials are similar because Sigma-Aldrich PET and waste PET have the same vibration peaks. In addition, the PET conversion yields for 1 g of coffee cup PET and 1 g of granular PET from Sigma-Aldrich were 92.5 % and 90.1 %, respectively. Thermal properties of waste PET from Appendix, Starbucks, and McDonald's were analyzed by differential scanning calorimetry (Fig. S19a). The glass transition temperature values (T_g) of all waste PET measured were 80-81 °C. T_g values provided information of amorphous region of PET. The cold crystallization and melting temperatures were 144-148 °C and 245-247 °C, respectively.

$$X_c = \frac{\Delta H_f - \Delta H_c}{\Delta H_f^0} \qquad \textbf{[Eq. S2]}$$

The degree of crystallinity (X_c) could be calculated using Eq. S2. ΔH_f is enthalpy of fusion and ΔH_c is the cold crystallization enthalpy. ΔH_f^0 value (140 J/g) is enthalpy of fusion when the PET sample is 100 % crystalline.[7] The waste PET from Appendix (0.0003), Starbucks (0.027), and McDonald's (0.018) had low crystallinity. Each PET sample and the mixture of three PET samples (Appendix : Starbucks : McDonald's = 1 : 1 : 1, weight ratio) were glycolyzed by K_2CO_3 catalyst. As shown in Fig. S19b, the conversion yields of waste PET from Appendix (92.5 %), Starbucks (88.5 %), McDonald's (93.4 %), and the mixture (92.5 %) were comparable. Based on these results, waste PET pieces from Appendix coffee cup were applied to establish the chemo-enzymatic depolymerization.

Screening of BHET hydrolytic enzymes suitable for chemo-enzymatic depolymerization

In the development of the chemo-enzymatic depolymerization, the establishment of a single enzymatic hydrolysis system is important because the current dual enzyme system, PETase, and MHETase, require high operation costs. Therefore, we attempt to develop a single enzyme system capable of BHET hydrolysis into TPA and EG. As shown in Fig. S4, the only esterase from *Bacillus subtilis* (Bs2Est) was able to completely hydrolyze BHET into TPA and EG while esterases from *P. barcinonensis, R. oryzae* and *M. populi* partially hydrolyzed BHET within 24 h. While esterase from *P. barcinonensis* hydrolyzed BHET to release MHET within 12 h, MHET hydrolytic activity was not observed.

Catalytic properties of Bs2Est activity

Enzyme kinetic parameters were determined to understand the enzyme properties toward two substrates, BHET and MHET. The K_M and V_{max} values toward BHET of Bs2Est were 8.84 (mM) and 5.99×10^4 (U/mg) while those toward MHET were 5.10 (mM) and 2.33 (U/mg), respectively (Table S1). When potential deleterious effects caused by excess EG or TPA disodium salt on hydrolysis activity of Bs2Est were examined by the addition of EG or TPA disodium salt with different concentrations (0-40 mM of EG or 0-16 mM of sodium TPA), we found that the enzyme activity was not reduced regardless of EG or TPA concentrations (Fig. S9 and S10). Based on the observations, BHET concentration increased to establish more efficient depolymerization.

Development of enzymatic hydrolysis of BHET using Bs2Est

The solubility of TPA in aqueous buffer solution has an important effect on BHET hydrolysis of Bs2Est. EG (up to 40 mM, Fig. S9) and TPA disodium salt (up to 16 mM, Fig. S9) did not inhibit BHET hydrolytic activity of Bs2Est. However, 8 mM BHET and 8 mM MEHT significantly inhibited the hydrolytic activity of Bs2Est (Fig. S11). The solubility of TPA was dependent on the type of buffer and TPA exhibited higher solubility in sodium phosphate buffer than in Tris-HCl. Only 6 mM BHET was fully solubilized in 50 mM Tris-HCl but 20 mM and 30 mM BHET was fully solubilized in 50 mM and 100 mM sodium phosphate buffer, respectively (Fig. S12). Therefore, 16 mM and 24 mM of BHET could be completely hydrolyzed into TPA and EG in 50 mM and 100 mM sodium phosphate buffer (Figs. S13d, S16b), respectively, while only 4 mM of BHET was hydrolyzed in 50 mM of Tris-HCl (Fig. S11a). Moreover, the BHET hydrolytic activity of Bs2Est was higher in 200 mM sodium phosphate buffer than in 50 mM sodium phosphate buffer with continuous titration by NaOH at pH 7.5 and in 100 mM sodium phosphate buffer although the final pH of the reaction mixtures in 100 mM and 200 mM sodium phosphate buffer was decreased to pH 6.53 and pH 6.92, respectively (Fig. S16). The hydrolytic activity of Bs2Est toward 20 mM BHET in 50 mM sodium phosphate buffer was compared with the known BHET-hydrolytic enzymes i.e., PETase and MHETase from *Idonella sakiensis*.[7b, c] PETase and MHETase exhibited lower TPA production yields from BHET (59.9% and 6.3%, respectively) than Bs2Est (99.9%) indicating PETase and MHETase are not suitable for one-pot enzymatic hydrolysis of the glycolyzed products (Fig. S14). To investigate the reason for the incomplete enzymatic hydrolysis of 24 mM BHET in 50 mM sodium phosphate buffer (Fig. S16a), the effect of BHET and acid form of TPA on the hydrolytic activity of Bs2Est toward MHET was investigated because MHET hydrolysis is rate-limiting in all Bs2Est-catalyzed reactions. Enzyme concentrations and residual activities of Bs2Est after 8 h incubation with 4, 24 mM BHET and after 8 h incubation with the acid form of TPA at different concentrations (0, 3, 6 mM) were compared (Fig. S17). Enzyme concentrations and residual activities of Bs2Est recovered from the reaction with 24 mM of BHET were 0.076 mg/mL and 28 mU/mL which were 3.6 fold and 2.7 fold less than those of Bs2Est recovered from the reaction with 4 mM of BHET, respectively (Fig. S17a). Moreover, it was observed that enzyme concentration and residual activity of Bs2Est after 8 h incubation with 6 mM acid form of TPA was reduced by 1.3-fold and 1.4-fold, respectively. Enzyme inhibition experiments reveal that acid form of TPA over maximal solubility, e.g. more than 24 mM of TPA in 50 mM sodium phosphate buffer causes a deleterious effect on the hydrolytic activity of Bs2Est (Fig. S13e,f). As shown in Fig. S19c, enzymatic hydrolysis of BHET mixture obtained from glycolysis of Appendix, Starbucks, McDonald's and the mixture of three PET bottles were conducted without purification (path 3). All the glycolysis mixtures were successfully

hydrolyzed from BHET, MHET and PET oligomers to TPA. The conversion yields of TPA obtained from Appendix (124.8 % [mol/mol]), Starbucks (125.1 % [mol/mol]), McDonalds (127.0 % [mol/mol]), and the mixture of three PET sampes (121.9 % [mol/mol]) were more than 100 % due to hydrolysis of MHET and PET oligomers.

Examination of PET oligomer-hydrolytic activity of Bs2Est

To investigate the reason for the excessive production of TPA, insoluble fractions in glycolyzed mixtures composed of PET oligomers (Fig. S20 and S21) with various degrees of polymerization (DP) (DP2-4) were reacted with Bs2Est. As shown in Fig. 2, the enzymatic reaction profile of path 3 exhibited rapid formation of MHET and gradual production of TPA, which was similar to that of the BHET hydrolysis reaction by using Bs2Est (path 1). MALDI-TOF mass spectrometry analysis of the enzymatic hydrolysates in path 3 was performed to elucidate how Bs2Est hydrolyzes PET oligomers. In Fig. 2b, the dimer was gradually hydrolyzed in enzyme reaction mixtures and was completely consumed after 10 h. On the other hand, hydrolysis of trimer and tetramer that exist as small proportion in PET oligomers was partially observed in MALDI TOF analysis using 2 U/mL of Bs2Est (Fig. 2b). This result indicates that those substrates are very poor substrates for Bs2Est in the buffer system (50-200 mM sodium phosphate) used in this study, implying that additional organic solvent systems will be required to improve enzymatic hydrolysis. Even with the addition of a low amount of enzyme, only the dimer disappeared without the formation of TPA-EG-TPA or EG-TPA-EG-TPA as possible hydrolytic products of exo-cleavage, and only MHET, TPA, and EG were detected using HPLC. BHET was not detected in the reaction mixtures because of the high catalytic efficiency of Bs2Est toward BHET (Table S1). As shown in Fig. S21, trimer and tetramer seemed to be not hydrolyzed into smaller molecules. This might be due to the low solubility of those compounds caused to reduce the enzyme activity as well as accessibility. PET oligomers with higher DP (trimer and tetramer) were detected until the end of the enzyme reaction. The formation profiles of TPA, EG, MHET, and BHET in the enzymatic hydrolysates of the PET oligomers were analyzed to investigate the hydrolysis mechanism of the PET oligomers, especially dimer. Based on these results, it can be assumed that Bs2Est catalyzes two sequential ester hydrolysis of the dimer in the initial reaction period i.e., cleavage of the internal ester bond in dimer and external bond in BHET (Fig. 2c). It seems that the Bs2Est enzyme cleaves an ester bond between MHET and BHET moieties in the dimer to release MHET and BHET. BHET formed can then be rapidly hydrolyzed into MHET and EG by Bs2Est with high catalytic efficiency toward BHET (k_{cat}/K_M: 2.37×10^4 [1/mM·s], Table S1). Then, MHET was completely hydrolyzed into TPA and EG with catalytic efficiency toward BHET (k_{cat}/K_M: 1.27 [1/mM· s], Table S1).

Molecular modeling simulation of Bs2Est

Molecular modeling simulation of Bs2Est supports the experimental results for the specific hydrolysis of the endo-ester bond in the dimeric substrate and for higher hydrolytic activity toward BHET than MHET. The binding pocket residues of Bs2Est formed π-π interaction (F314), cation-π interaction (H399) with an aromatic ring, and hydrogen bonds (G106, A107, Y109, Y118 and E188) with ester, hydroxyl, and carboxylic groups of the substrates (Fig. 2d, 2e, and 2f). In the docking pose of the dimeric substrate (EG-TPA-EG-TPA-EG), the chain corresponding to MHET (TPA-EG) dwelled in the small pocket and the chain corresponding to BHET (EG-TPA-EG) lay toward the large pocket. The aromatic rings of the dimeric substrate had a π-π interaction with F314 (BHET moiety) and a π-cation interaction with H399 (MHET moiety), and the oxyanion hole was stabilized by the proximal G106 and A107 backbone nitrogen (Fig. 2d). Thus, the binding distance between the catalytic S189 side-chain oxygen and the endo-ester carbon (3.0 Å) was close to initiate a nucleophilic attack.[8] However, the docking pose of exo-cleavage favorable conformation did not form oxyanion stabilizing interactions and the binding distance (3.6 Å) was not close enough for the catalysis. This result indicates that the dimeric substrate binds in the endo-cleavage favorable conformation for direct release of MHET and BHET. The same method was applied to BHET and MHET. In the docking pose of BHET, the benzene ring formed π-π interaction with F314, the oxyanion hole was stabilized by hydrogen bonds with G106 and A107, and both terminal hydroxyl groups had hydrogen bonds with Y109 and E188 (Fig. 2e). The binding distance between the catalytic S189 and the ester carbon was (3.6 Å). In contrast to BHET, MHET (black in Fig. 2f) maintained π-π interaction with F314 but the hydrogen bonds in the oxyanion hole were disrupted and the hydroxyl group formed new hydrogen bonds with the backbones of F274 and F275, leading to a far distance, i.e., unable to catalyze, between the catalytic S189 and the ester carbon. Most docking poses of MHET exhibited similar less favorable binding between the enzyme-substrate complexes and in only few docking poses, MHET (green in Fig. 2f) formed the π-π interaction, the hydrogen bond with E188 to form a close distance between the catalytic S189 and the ester carbon (3.3 Å) for favorable binding. Thus, molecular docking simulations elucidate that Bs2Est exhibited the preferred hydrolytic activity toward BHET by forming specific interactions including π-π interaction, π-cation interaction, and hydrogen bond but, further crystallographic experiments with substrate analogs are required to fully understand the mode of action of Bs2Est.

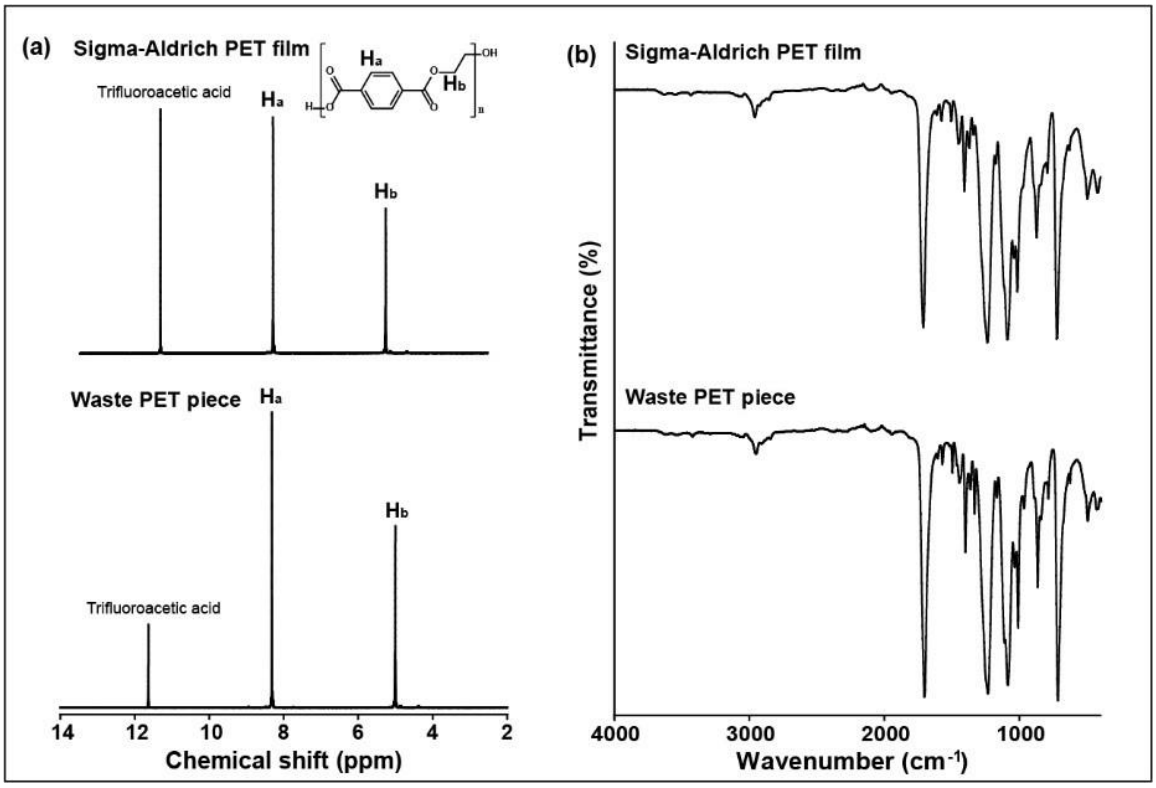

Figure S1. (a) ^{1}H-NMR and (b) FT-IR spectra of Sigma-Aldrich PET film and waste PET pieces. Before the reaction, the chemical properties of the waste PET piece and Sigma-Aldrich PET film were compared.

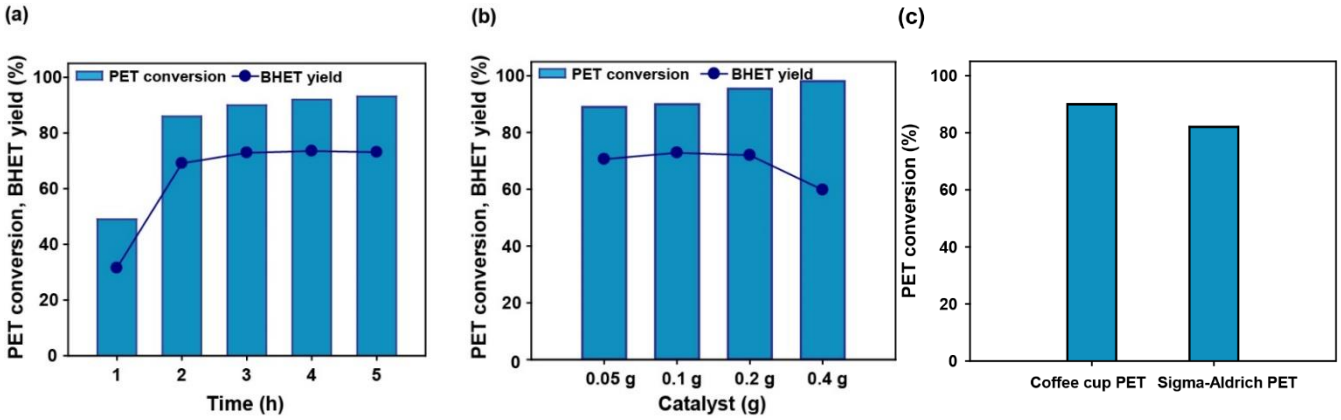

Figure S2. Optimization of glycolysis using K_2CO_3 as a catalyst. (a) Effect of reaction time on the yield of BHET and (b) effect of K_2CO_3 catalyst loading on the yield of BHET. (c) The PET conversion yields (%) for coffee cup PET and Sigma-Aldrich PET. PET conversion yields and BHET yield were calculated by [Eq. 1], [Eq. 2] and [Eq. 3], respectively.

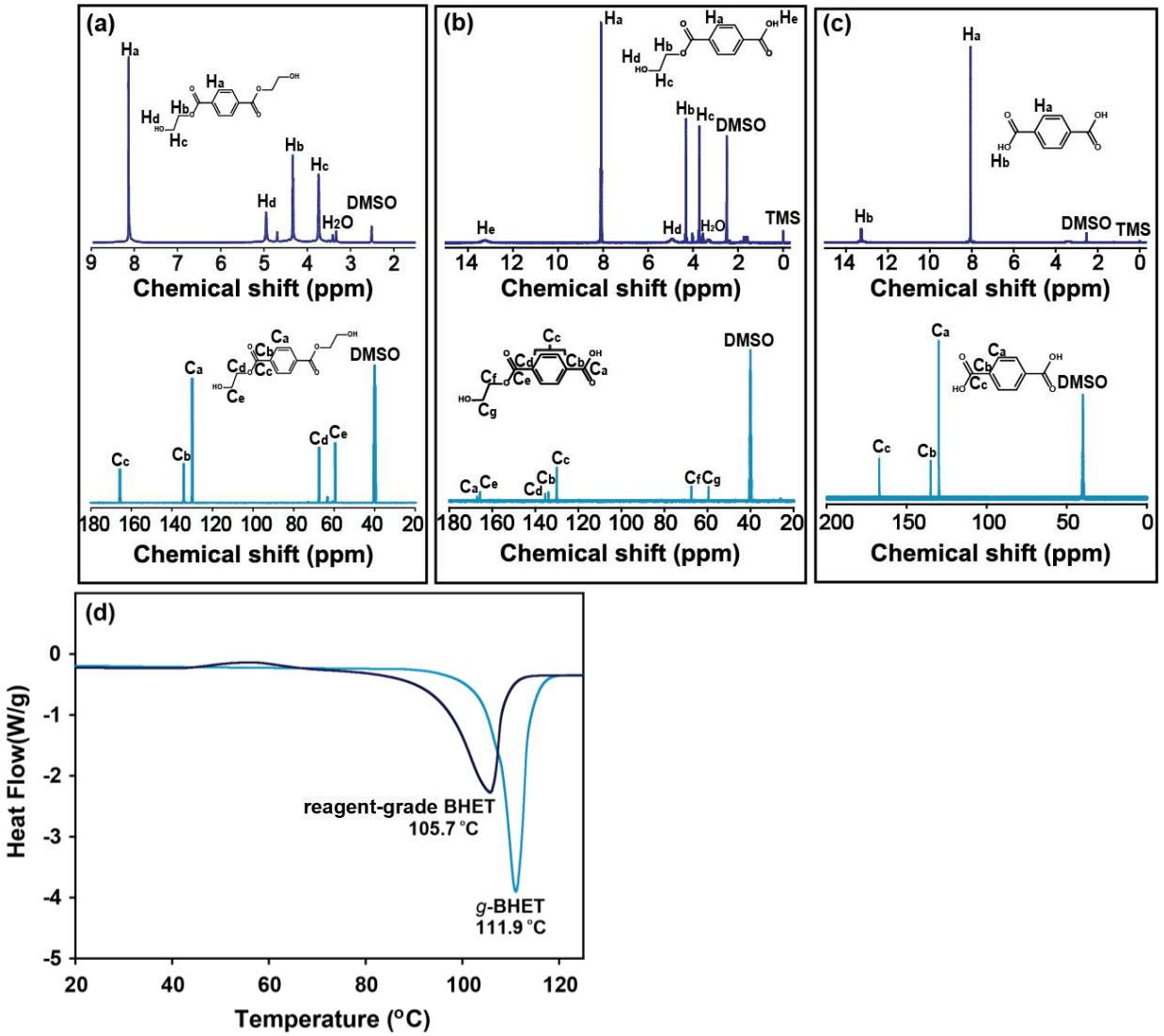

Figure S3. ^{1}H and ^{13}C-NMR spectra of reagent-grade (a) BHET, (b) MHET, (c) TPA, and (d) DSC curves of reagent-grade BHET and *g*-BHET. From these results, *g*-BHET was proved to be almost identical to reagent-grade BHET.

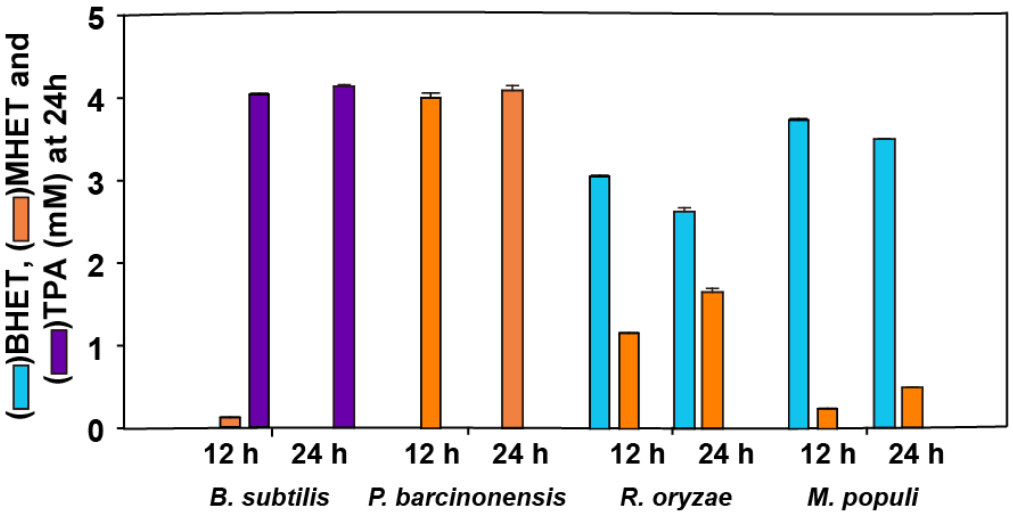

Figure S4. The hydrolysis test of BHET to TPA with commercial esterase. The enzymatic reaction was conducted on 4 mM BHET using 1 U/mL of esterase. The reactions were performed at 30 °C and 1000 rpm for 24 h using 1 U/mL of enzyme in 50mM Tris-HCl buffer (pH 7.5)

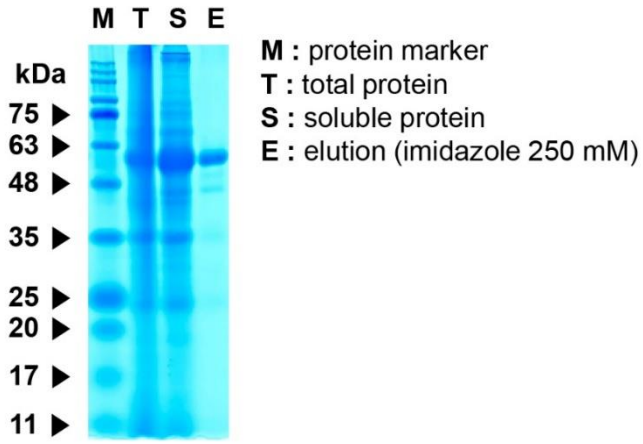

Figure S5. SDS-PAGE of Bs2Est enzyme, M, marker; T, total protein; S, crude enzyme; E, purified recombinant protein. For the standard, PM2700 ExcelBand TM 3-color Broad Range Protein Marker SMOBIO® (Taiwan) was used.

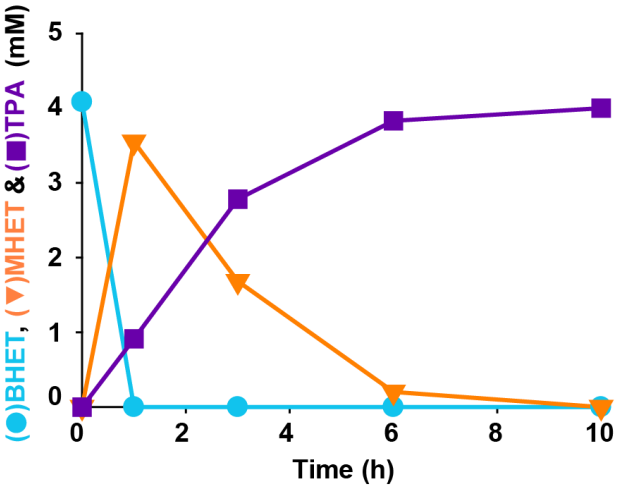

Figure S6. The time course profiling of the enzymatic reaction of BHET by the addition of 1 U/mL of Bs2Est. The reactions were performed at 30 °C and 1000 rpm using 4 mM BHET for 10 h in 50 mM Tris-HCl (pH 7.5). The symbol of circle, inverted triangle, and square represent BHET, MHET, and TPA, respectively.

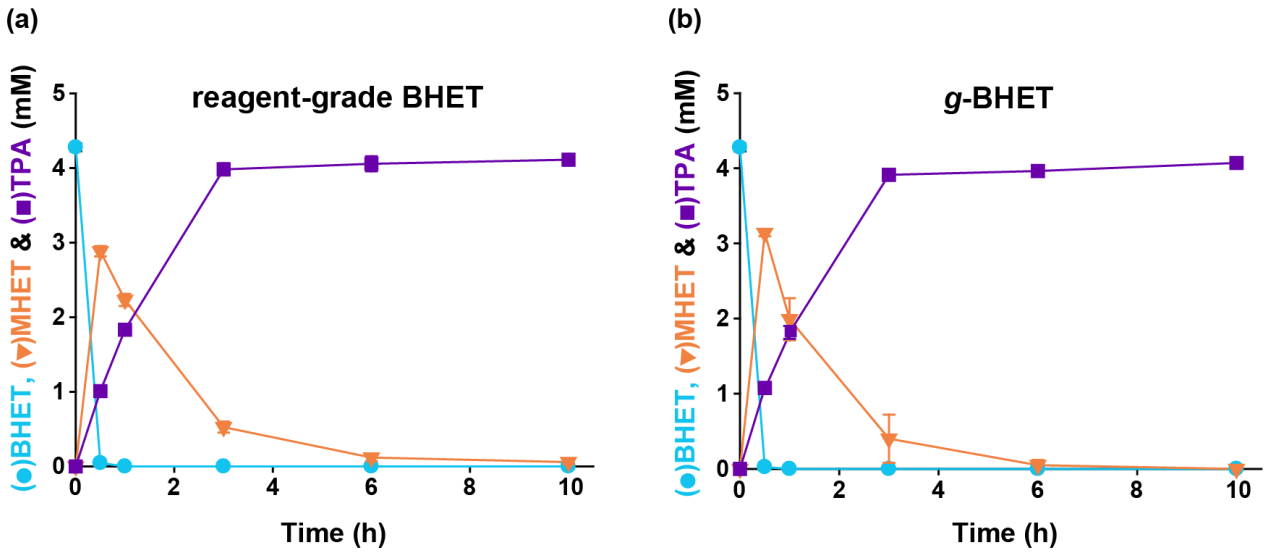

Figure S7. Comparison of enzymatic reactions using (a) reagent-grade BHET (Sigma-Aldrich) and (b) *g*-BHET (recrystallized BHET from glycolyzed mixture) using 4 mM BHET in 50 mM Tris-HCl buffer (pH 7.5) at 30 °C and 1000 rpm by the addition of 2 U/mL of Bs2Est.

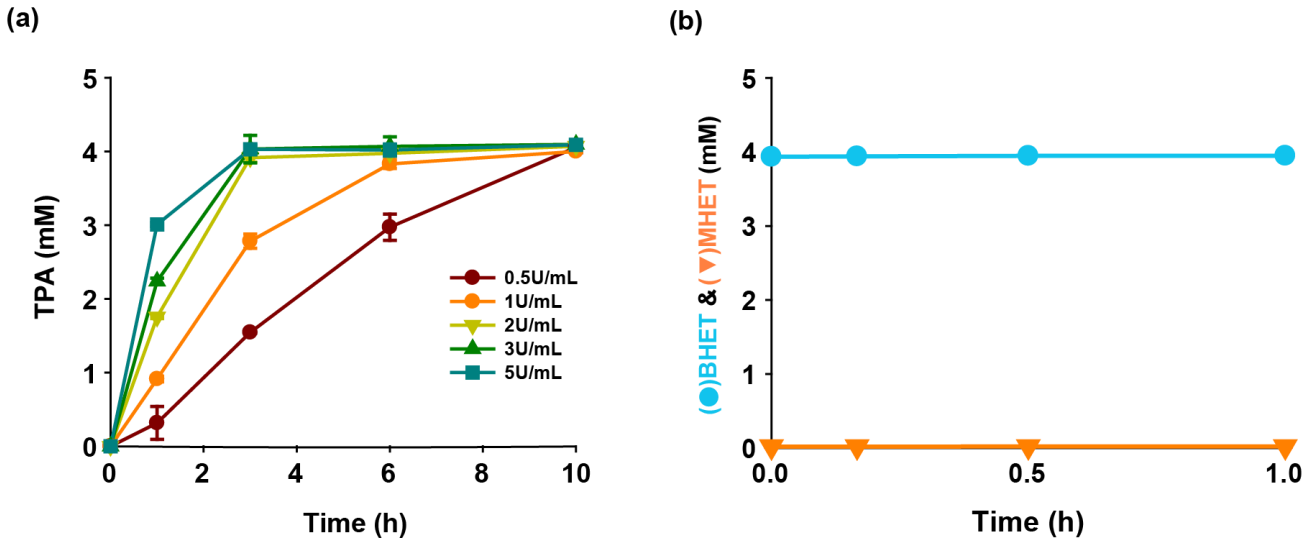

Figure S8. (a) Optimization of Bs2Est loading amount. The enzymatic reaction was performed on 4 mM BHET using 0.5-5 U/mL of Bs2Est at 30 °C and 1000 rpm in 50 mM Tris-HCl buffer (pH 7.5). (b) Effect of methanol quenching. 19 volumes of methanol were added to terminate the enzymatic reaction.

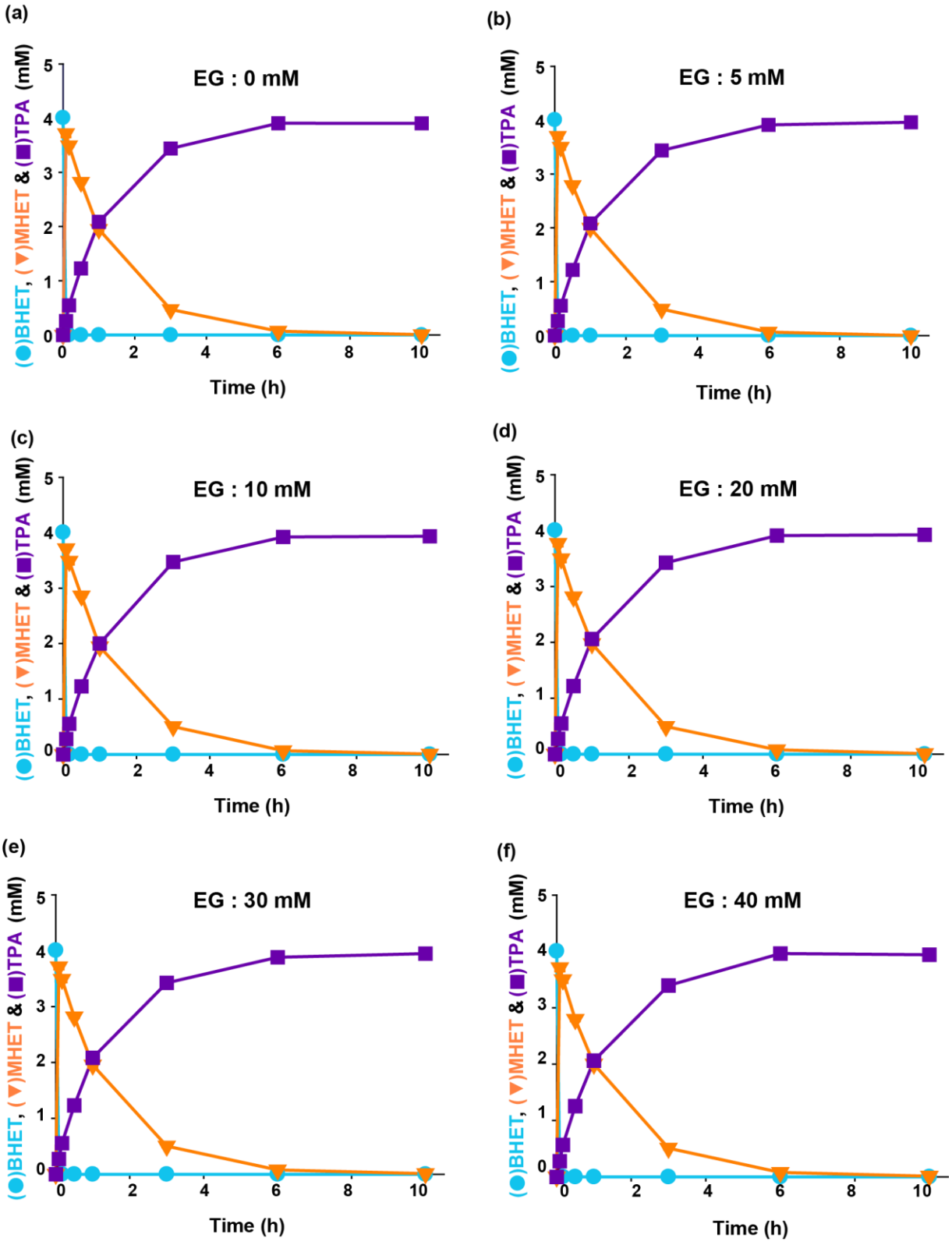

Figure S9. Effect of excess EG on the enzyme reaction rate. The reactions were performed on the different concentration of (a) 0 mM (b) 5 mM (c) 10 mM (d) 20 mM (e) 30 mM and (f) 40 mM EG using 2 U/mL of Bs2Est at 30 ^{o}C and 1000 rpm in 50 mM Tris-HCl buffer (pH 7.5).

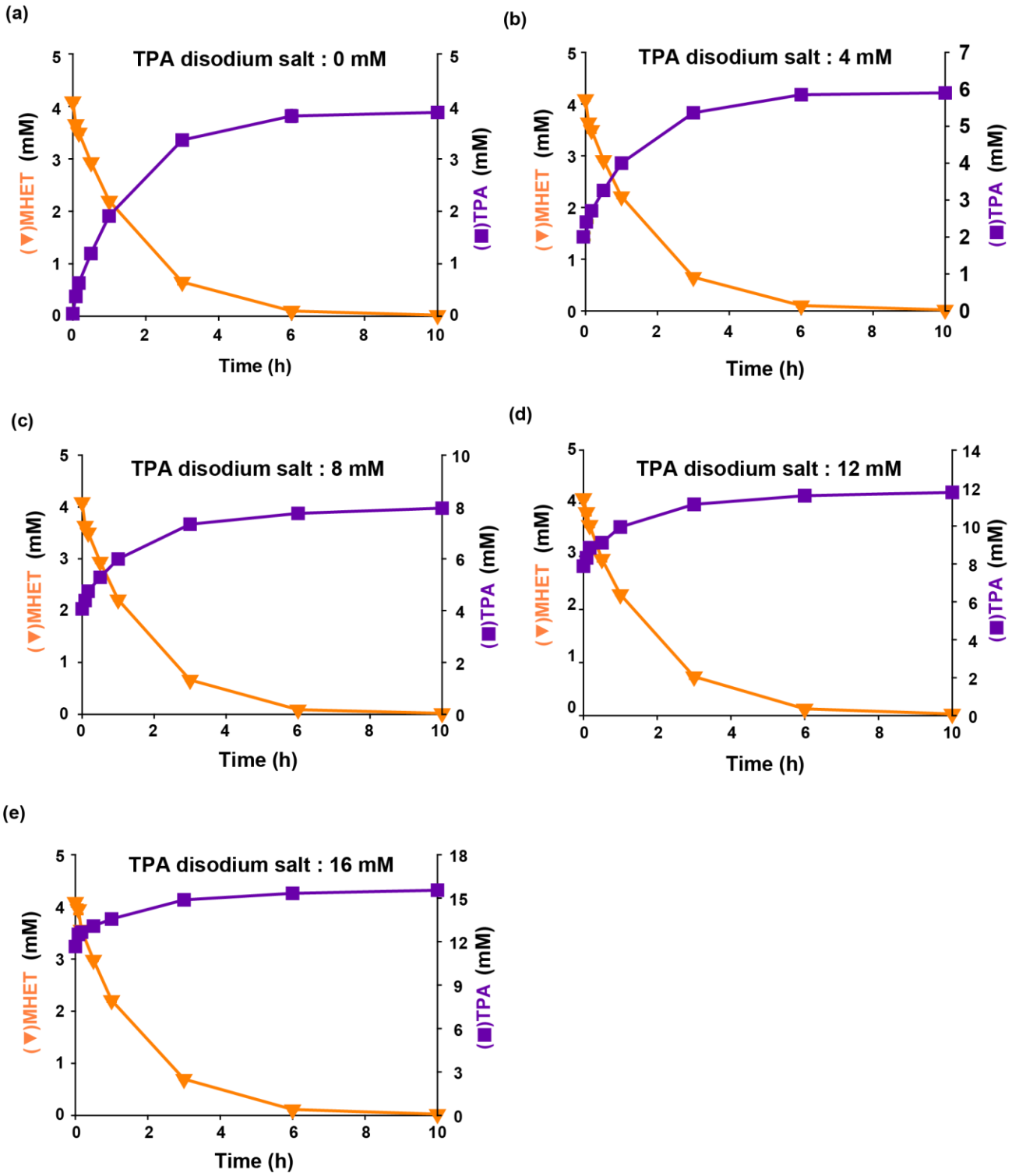

Figure S10. Effect of excess TPA disodium salt on the enzymatic reaction rate. The reactions were performed at different concentrations of (a) 0 mM (b) 4 mM (c) 8 mM (d) 12 mM (e) 16 mM TPA using 2 U/mL of Bs2Est loading at 30 °C and 1000 rpm in 50 mM Tris-HCl buffer (pH 7.5).

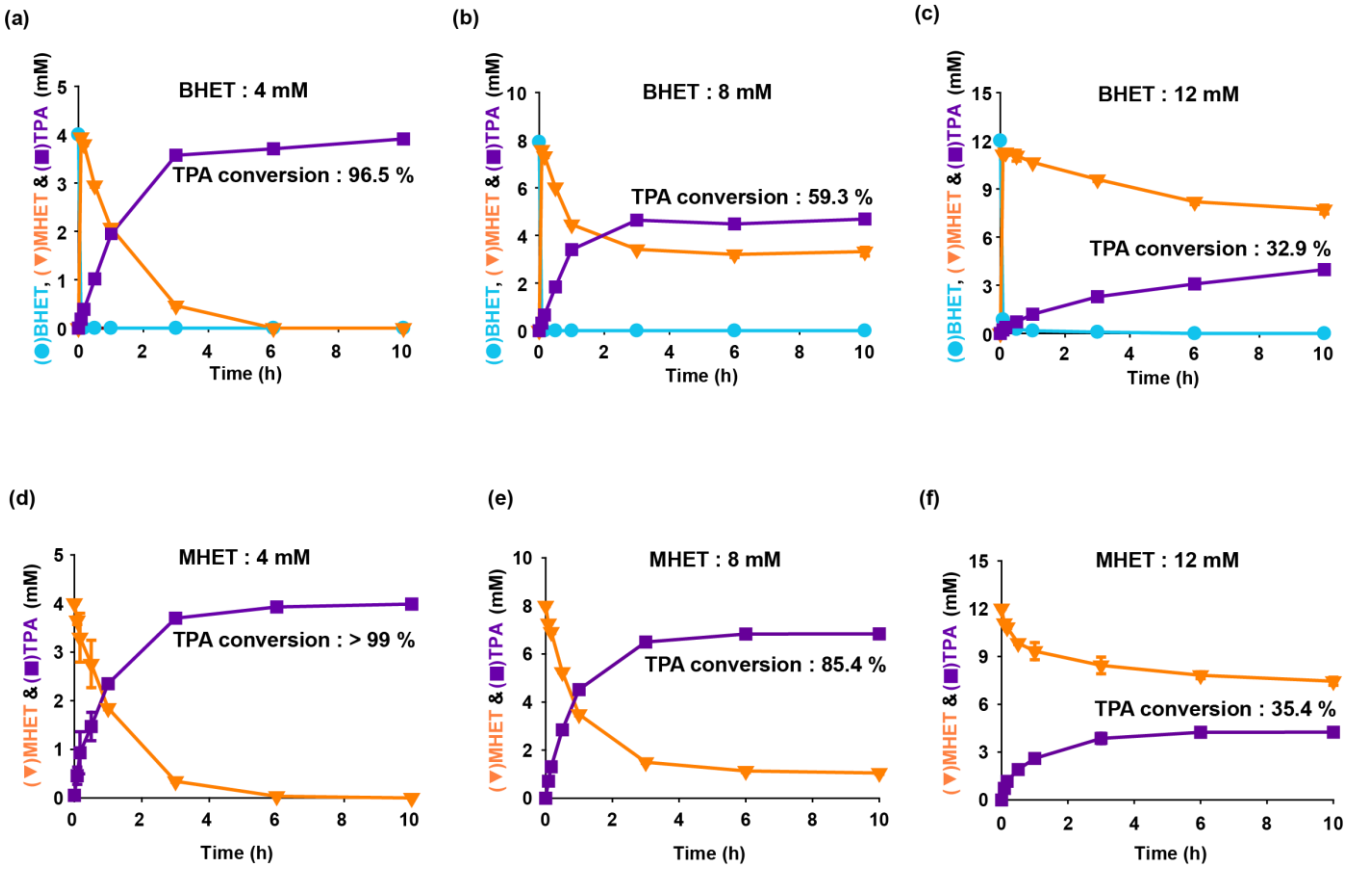

Figure S11. Change of the enzymatic reaction profiles at (a) 4 mM, (b) 8 mM, (c) 12 mM of BHET and (d) 4 mM, (e) 8 mM, (f) 12 mM of MHET concentration in 50 mM Tris-HCl buffer (pH 7.5). The reactions were performed at 30 °C and 1000 rpm for 10 h

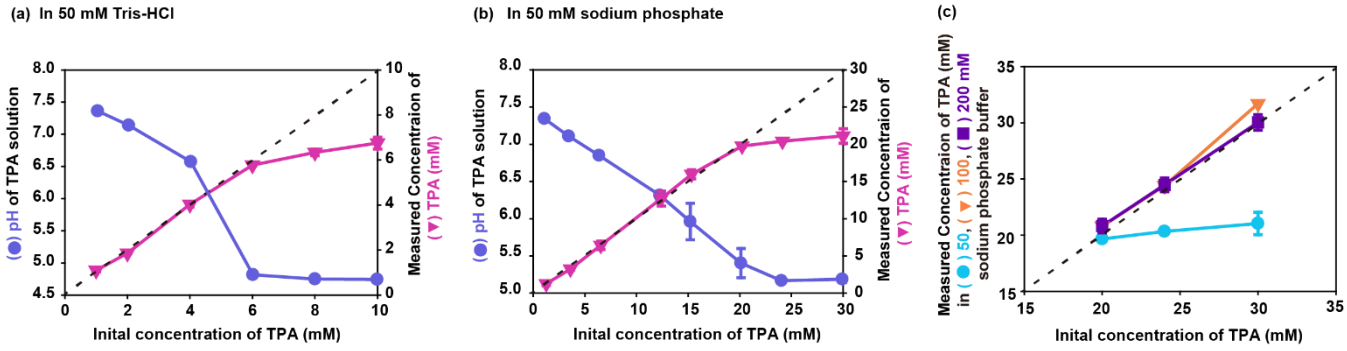

Figure S12. Solubility changes of TPA in (a) 50mM Tris HCl and (b) 50 mM sodium phosphate buffer. (c) The measured concentration of TPA (mM) at initial concentrations of 20, 24, and 30 mM TPA in 50, 100, and 200 mM sodium phosphate buffer, respectively.

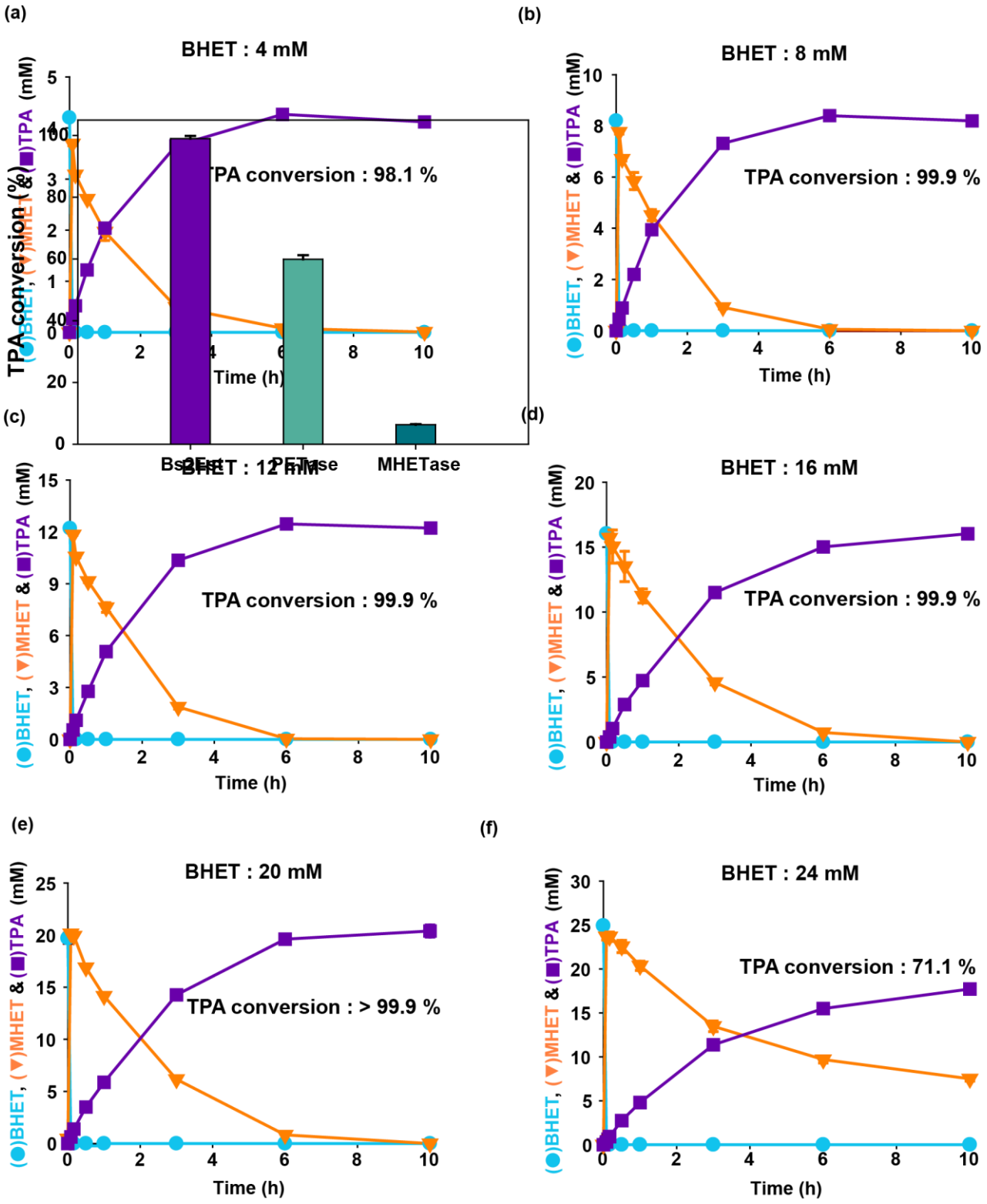

Figure S13. The enzymatic profiles according to the BHET concentration of (a) 4 mM, (b) 8 mM, (c) 12 mM, (d) 16 mM, (e) 20 mM, and (f) 24 mM in 50 mM sodium phosphate buffer (pH 7.5). The enzymatic reactions were conducted at 30 °C and 1000 rpm.

Figure. S14. Comparison of the hydrolytic acitivities of (a) Bs2Est, (b) PETase, and (c) MHETase toward BHET. The reactions were conducted at 20 mM BHET and 30 °C for 10 h using equal concentration (0.55 mg/mL) of Bs2Este, PETase and MHETase in 50 mM sodium phosphate buffer.

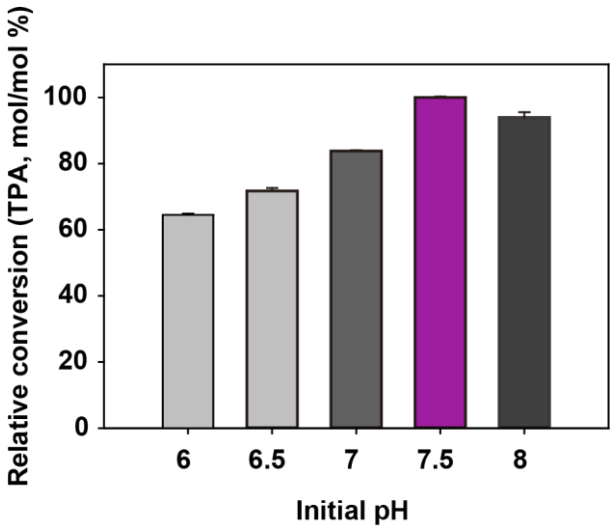

Figure S15. Effect of initial pH. The enzymatic reactions were performed on 2 mM of MHET using 2 U/mL of Bs2Est for 3 h. The reaction mixture was stirred at 1000 rpm and 30 °C.

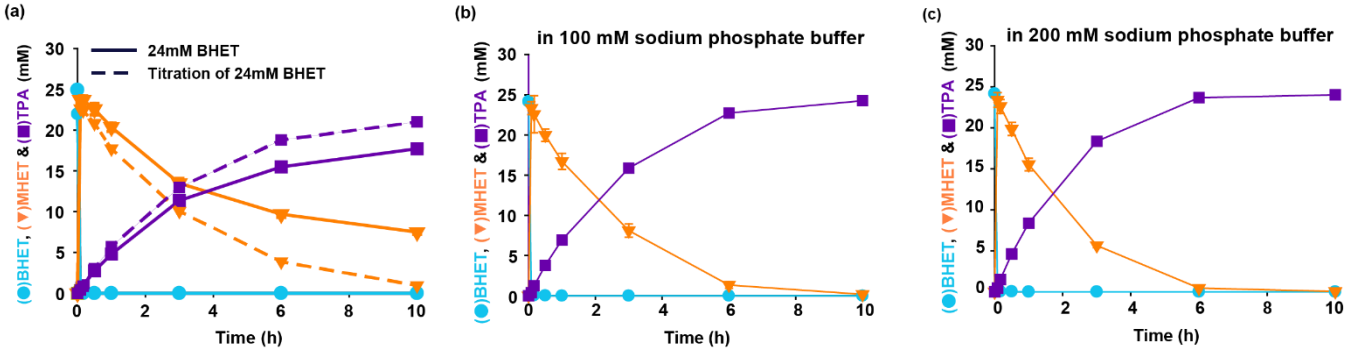

Figure S16. Enzymatic reaction of 24 mM BHET using 2 U/mL of Bs2Est in (a) 50 mM sodium phosphate buffer with continuous titration by NaOH at pH 7.5 (b) 100 mM, and (c) 200 mM sodium phosphate buffer. The reaction mixtures were stirred at 1000 rpm and 30 °C.

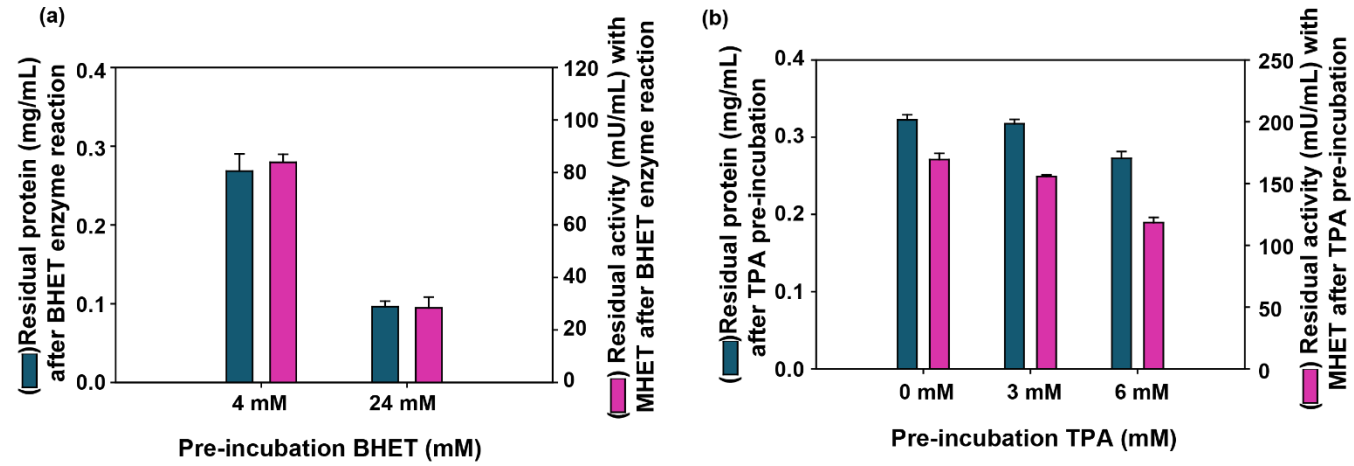

Figure S17. Enzyme concentration and residual activity after 8 h pre-incubation on (a) 4 and 24 mM BHET in 50 mM sodium phosphate buffer (pH 7.5) and (b) 0, 3 and 6 mM TPA in 50 mM Tris-HCl buffer. The enzymatic reactions were performed at 30 °C and 1000 rpm in 50 mM sodium phosphate buffer containing 2 mM of MHET and 0.5 U/mL of Bs2Est (0.32 mg/mL).

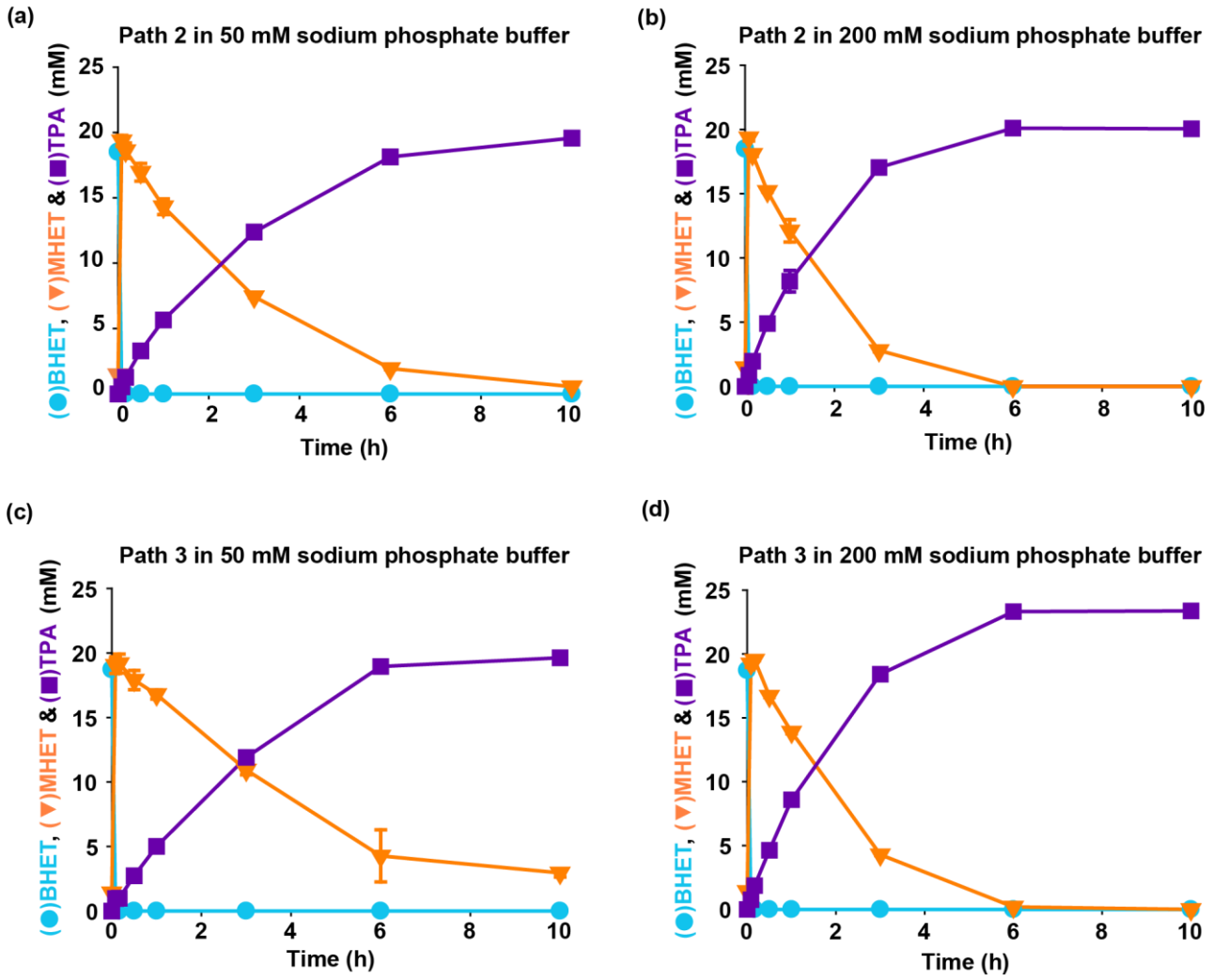

Figure S18. Profiling of enzymatic reaction using glycolyzed products (Path 2 (a, b); after filtration and Path 3 (c,d); without any purification) in (a, c) 50 mM (b, d) 200 mM sodium phosphate buffer. Path 2 and Path 3 reactions were performed at 30 °C and 1000 rpm using 2 U/mL of Bs2Est.

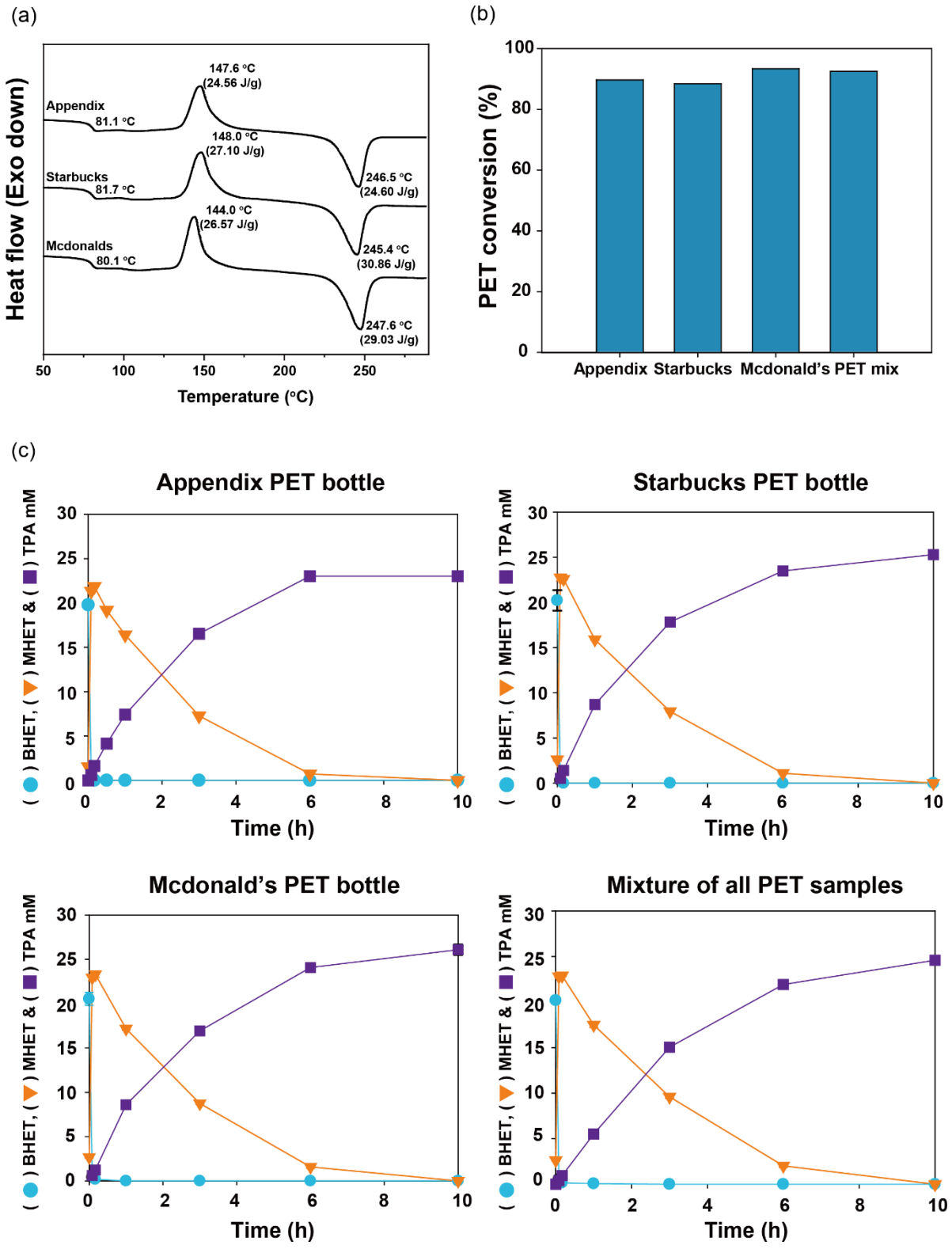

Figure S19. Chemo-enzymatic depolymerization of PET samples. (a) DSC curves of waste PET from Appendix, Starbucks, and McDonald's. (b) The PET conversion yields (%) and (c) enzymatic hydrolysis profiles on the different substrate from Appendix, Starbucks, and McDonald's and the mixture of three PET samples (Appendix : Starbucks : McDonald's =1 : 1 : 1, weight ratio). The reactions were performed at 30 °C and 1000 rpm in 100 mM sodium phosphate buffer by the addition of 2 U/mL of Bs2Est.

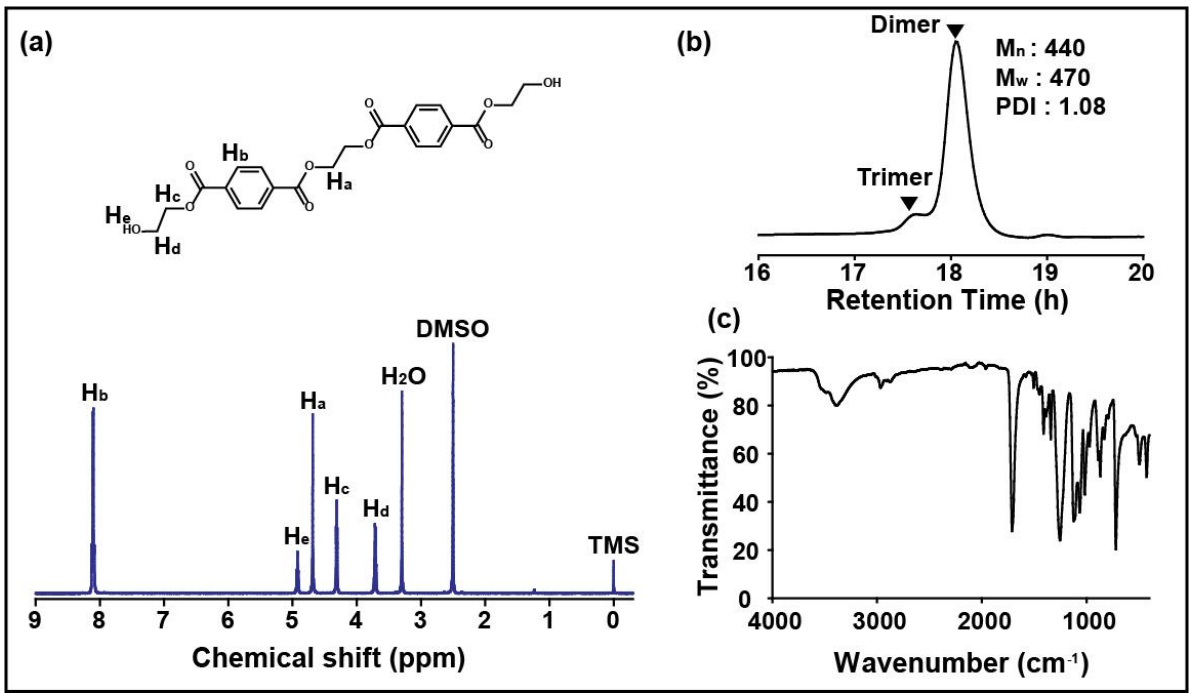

Figure S20. (a) ^{1}H-NMR spectrum, (b) GPC graph and (c) FT-IR spectrum of oligomer. As shown in Fig S21e, the main peak was identified as a dimer in MALDI-TOF.

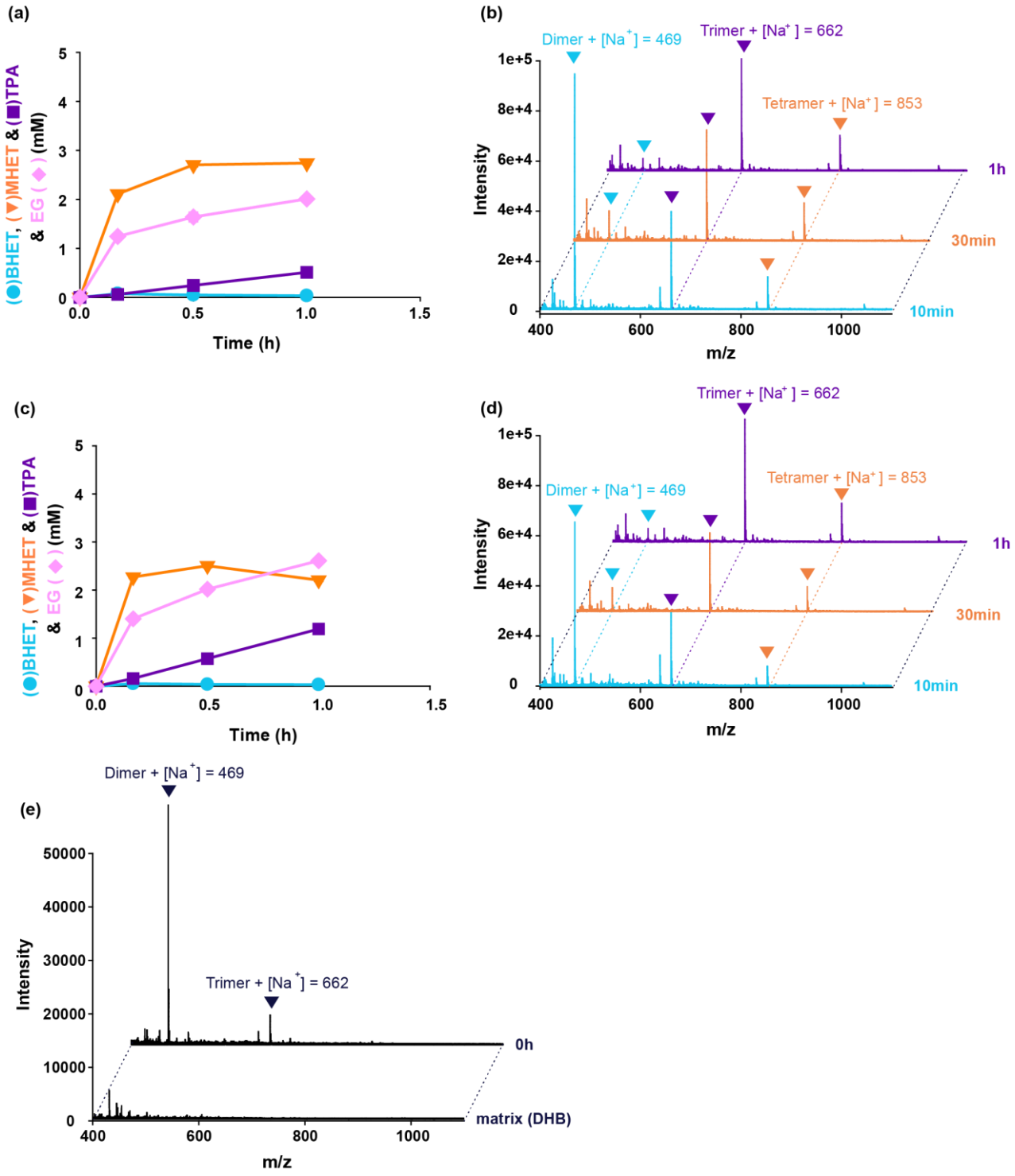

Figure S21. Profiling of enzymatic reactions (a and c) and chromatogram of MALDI-TOF (b and c) when 0.5 U/mL (a and b) and 1 U/mL (c and d) were reacted with 1 g/L of PET oligomers The reactions were conducted at 30 °C and 1000 rpm in 50 mM Tris-HCl buffer (pH 7.5). (e) MALDI-TOF of PET oligomers and matrix.

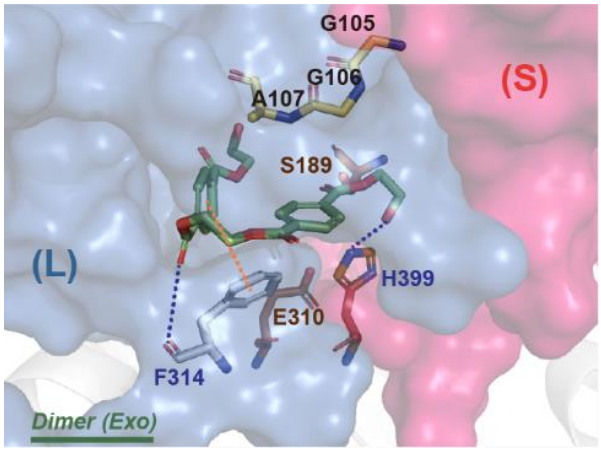

Figure S22. Hypothetical binding mode of the dimer in the hydrolysis of the exo-ester bond. In order to hydrolyze the exo-ester bond of the dimer, the bond must be oriented adjacent to the S189, and most part of the dimer has to be forced into the large pocket, adopting an unstable V-shaped structure protruding toward the entrance of the active site. The oxyanion cannot be stabilized in this configuration.

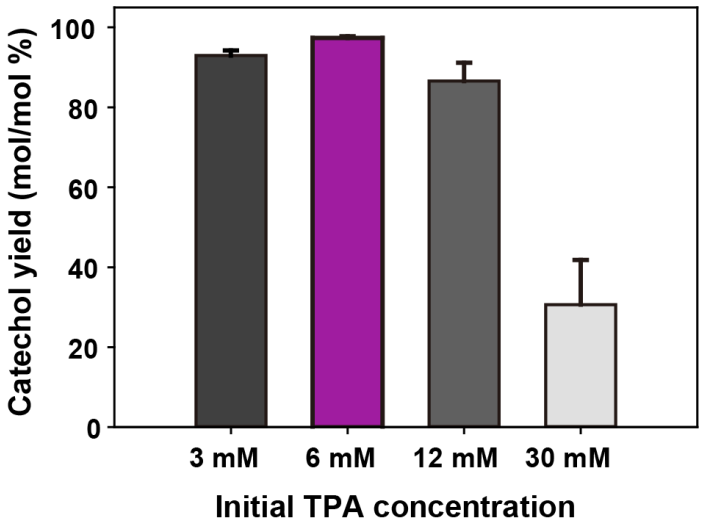

Figure S23. Optimal TPA loading for bioconversion reaction. The catechol yields of 3, 6, 12, and 30 mM of TPA are 93, 97, 87, and 42%, respectively. The ratio was calculated as final catechol (mM) / Initial TPA (mM). Bioconversion reactions were performed at 30 °C and 250 rpm for 20 h.

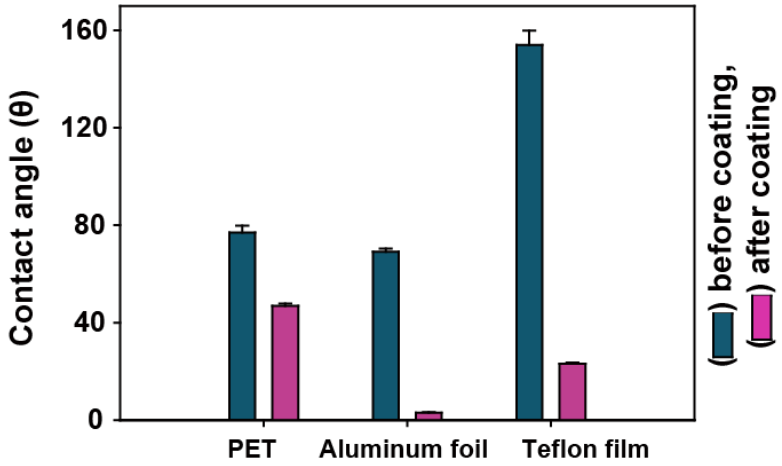

Figure S24. Contact angle (θ) before and after catechol coating.

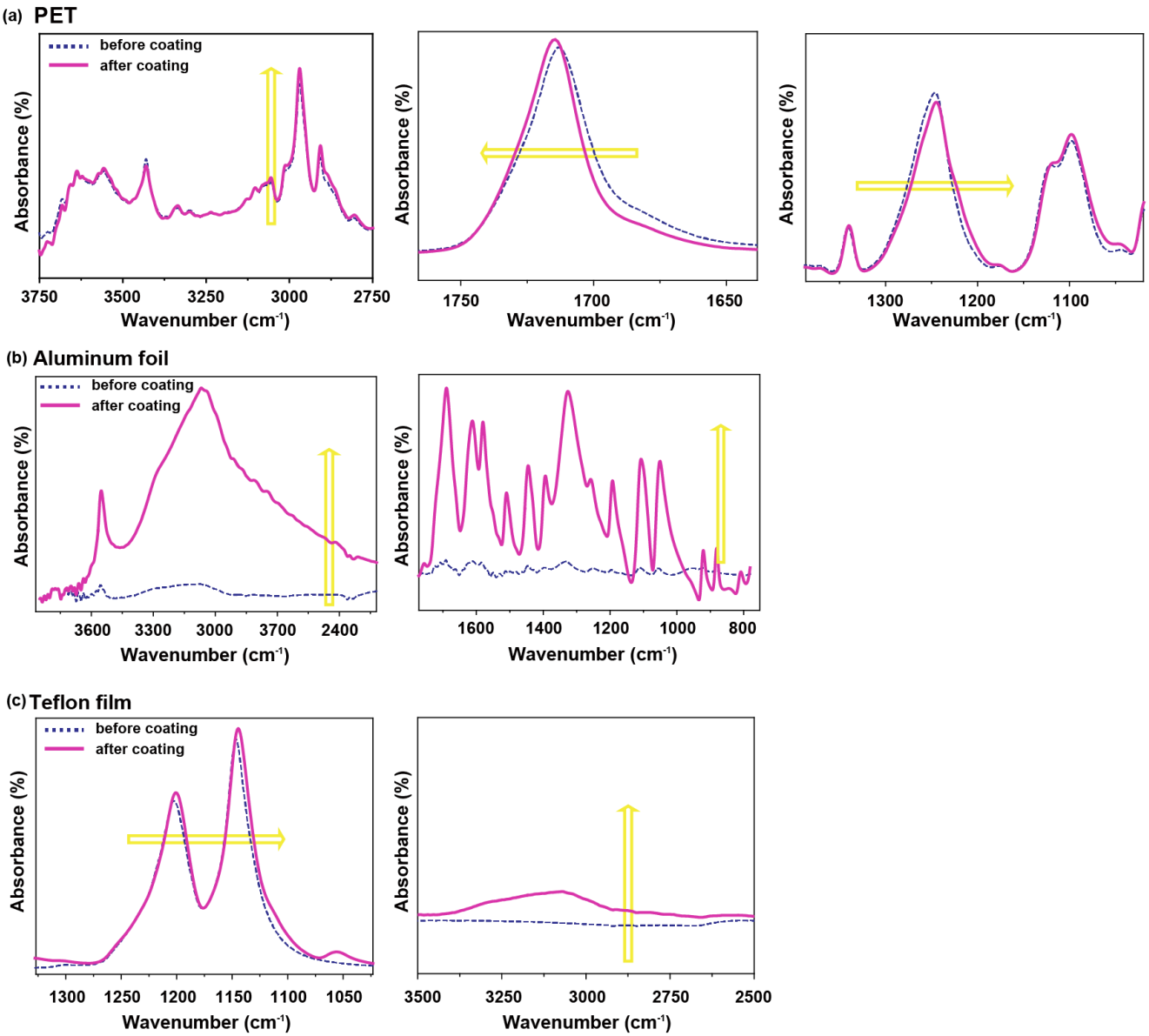

Figure S25. Absorbance (%) before and after catechol coating at (a) PET, (b) aluminum foil, and (c) Teflon film.

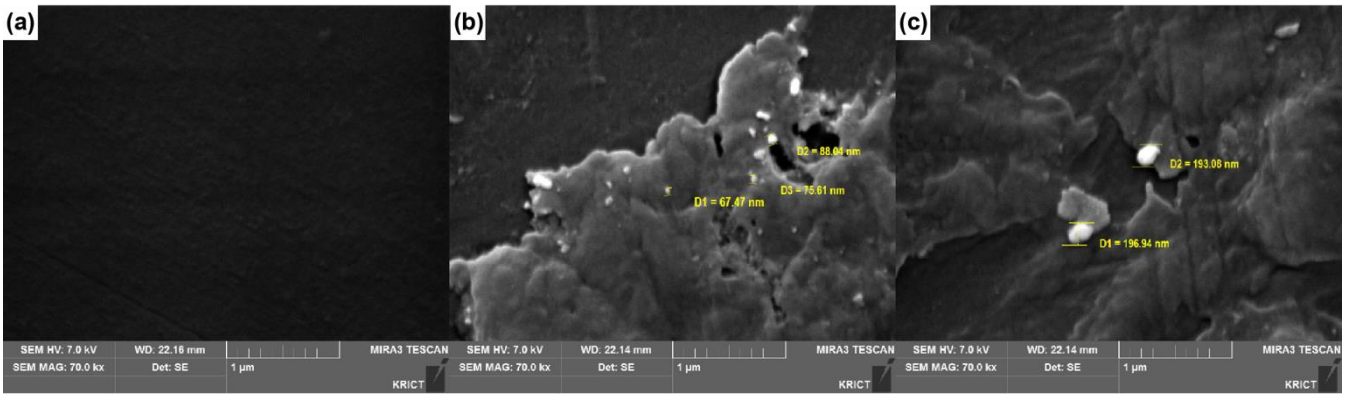

Figure S26. SEM images of (a) pristine and (b, c) silver nanoparticle-coated PET. Silver nanoparticles with the size of 60-200 nm were observed on the surface.

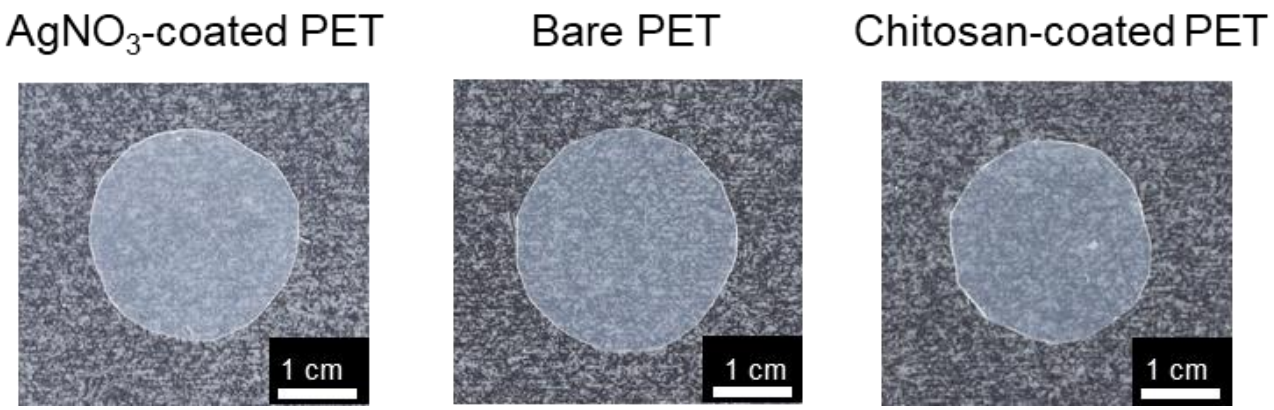

Figure S27. Images of bare PET, $AgNO_3$-coated PET, and chitosan-coated PET without the coating of catechol as an adherent layer.

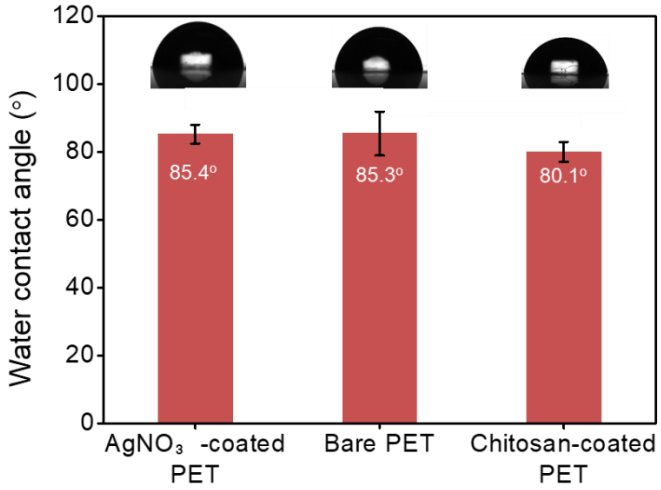

Figure S28. Contact angle data of bare PET, $AgNO_3$-coated PET, and chitosan-coated PET without the coating of catechol as an adherent layer. The data are mean and standard deviation of triplicate samples.

Table S1. Enzyme kinetics of Bs2Est towards (a) BHET and (b) MHET in 50 mM sodium phosphate buffer.

Substrate[a]	K_M (mM)	V_{max} (U/mg)	k_{cat} (1/s)	k_{cat}/K_M (1/mM·S)
BHET	8.84	5.99×10^4	2.10×10^5	2.37×10^4
MHET	5.10	2.33	6.46	1.27

[a] The enzymatic reactions were performed on 0.5–20 mM of BHET or 0.5–14 mM of MHET at 30 °C and 1000 rpm in 50 mM sodium phosphate buffer (pH 7.5).

Table S2. Nucleic acid sequences of genes used in this study

Gene	UniProtKB Accession number	Sequence
tphAa	Q3C1D2	ATGAACCACCAGATCCATATCCACGACTCCGATATCGCGTTCCCCTGCGCGCCCGGGCA ATCCGTACTGGATGCAGCTCTGCAGGCCGGCATCGAGCTGCCCTATTCCTGCCGCAAAG GTAGCTGTGGCAACTGTGCGAGTACGCTGCTCGACGGAAATATTGCCTCCTTCAATGGC ATGGCCGTGCGAAACGAACTCTGCGCCTCGGAACAAGTGCTGCTGTGCGGCTGCACTG CAGCCAGCGATATACGTATCCACCCGAGCTCCTTTCGCCGTCTCGACCCGGAAGCCCGA AAACGTTTTACGGCCAAGGTGTACAGCAATACACTGGCGGCACCCGATGTCTCGCTGCT GCGCCTGCGCCTGCCTGTGGGCAAGCGCGCCAAATTTGAAGCCGGCCAATACCTGCTG ATTCACCTCGACGACGGGGAAAGCCGCAGCTACTCTATGGCCAATCCACCCCATGAGA GCGATGGCATCACATTGCATGTCAGGCATGTACCTGGTGGTCGCTTCAGCACTATCGTT CAGCAGTTGAAGTCTGGTGACACATTGGATATCGAACTGCCATTCGGCAGCATCGCACT GAAGCCTGATGACGCAAGGCCCCTGATTTGCGTTGCGGGTGGCACGGGATTTGCGCCC ATTAAATCCGTTCTTGATGACTTAGCCAAACGCAAGGTTCAGCGCGACATCACGCTGAT CTGGGGGGCTCGCAACCCCTCGGGCCTGTATCTTCCTAGCGCCATCGACAAGTGGCGC AAAGTCTGGCCACAGTTTCGCTACATTGCAGCCATCACCGACCTAGGCGATATGCCTGC GGATGCTCACGCAGGTCGGGTGGATGACGCGCTACGCACTCACTTTGGCAACCTGCAC GATCATGTGGTGCACTGCTGTGGCTCACCAGCTCTGGTTCAATCAGTGCGCACAGCCGC TTCCGATATGGGCCTGCTTGCACAGGACTTCCACGCGGATGTTTTTGCGACAGGCCCGA CTGGTCACCACTAG
tphAb	Q3C1D5	ATGCAAGAATCCATCATCCAGTGGCATGGGGCCACTAATACGCGCGTGCCTTTTGGTAT CTATACCGACACAGCCAATGCTGATCAGGAACAGCAGCGCATCTATCGCGGCGAGGTC TGGAACTACTTGTGCCTGGAATCTGAAATTCCCGGGGCCGGTGATTTCCGCACTACCTT TGCCGGTGAAACACCGATAGTTGTCGTACGGGATGCCGACCAGGAAATCTACGCCTTC GAGAACCGCTGCGCGCATCGCGGCGCTCTCATCGCTCTGGAGAAATCGGGCCGTACGG ATAGTTTCCAGTGCGTCTATCACGCCTGGAGCTACAACCGACAGGGAGATCTGACCGG CGTTGCCTTCGAGAAAGGTGTCAAGGGCCAGGGTGGCATGCCGGCCTCATTCTGCAAA GAAGAGCATGGCCCGCGCAAGCTCCGCGTGGCTGTCTTTTGCGGTTTGGTCTTTGGCA GTTTTTCCGAGGACGTGCCCAGCATTGAGGATTACCTTGGCCCTGAGATTTGCGAGCGC ATAGAGCGCGTGCTGCACAAGCCCGTAGAAGTCATCGGTCGCTTCACGCAAAAGCTGC CTAACAACTGGAAGCTCTACTTCGAGAACGTGAAGGACAGCTATCACGCCAGCCTCCTG CATATGTTCTTCACCACCTTCGAGCTGAATCGCCTCTCACAAAAAGGCGGTGTCATCGTC GACGAGTCGGGTGGCCACCATGTGAGCTATTCCATGATCGATCGCGGCGCCAAAGACG ACTCGTACAAGGACCAGGCCATCCGCTCCGACAACGAGCGTTACCGGCTCAAAGATCC TAGCCTTCTAGAGGGCTTTGAGGAGTTCGAGGACGGCGTGACCCTGCAGATCCTTTCT GTGTTCCCTGGCTTTGTGCTGCAGCAGATTCAGAACAGCATCGCCGTGCGTCAGTTGCT GCCCAAGAGCATCTCCAGCTCGGAACTCAACTGGACCTATCTTGGCTATGCAGATGACA GTGCCGAGCAACGCAAGGTCAGACTCAAACAGGCCAACCTTATCGGCCCGGCCGGATT CATTTCCATGGAAGACGGAGCTGTCGGTGGATTCGTGCAGCGTGGCATCGCAGGCGCT GCCAACCTTGATGCAGTCATCGAGATGGGCGGAGACCACGAAGGCTCTAGCGAGGGC CGCGCCACGGAAACCTCGGTACGCGGCTTTTGGAAGGCCTACCGCAAGCATATGGGAC AGGAGATGCAAGCATGA
tphAc	Q3C1D4	ATGATCAATGAAATTCAAATCGCGGCCTTCAATGCCGCCTACGCGAAGACCATAGACA GTGATGCAATGGAGCAATGGCCAACCTTTTTCACCAAGGATTGCCACTATTGCGTCACC

		AATGTCGACAACCATGATGAGGGACTTGCTGCCGGCATTGTCTGGGCGGATTCGCAGG ACATGCTCACCGACCGAATTTCTGCGCTGCGCGAAGCCAATATCTACGAGCGCCACCGC TATCGCCATATCCTGGGTCTGCCTTCGATCCAGTCAGGCGATGCAACACAGGCCAGCGC TTCCACTCCGTTCATGGTGCTGCGCATCATGCATACAGGGGAAACAGAGGTCTTTGCCA GCGGTGAGTACCTCGACAAATTCACCACGATCGATGGCAAGTTACGTCTGCAAGAACG CATCGCGGTTTGCGACAGCACGGTGACGGACACGCTGATGGCATTGCCGCTATGA
tphB	Q3C1D3	ATGACAATAGTGCACCGTAGATTGGCTTTGGCCATCGGCGATCCCCACGGTATTGGCCC AGAAATCGCACTGAAAGCTCTCCAGCAGCTGTCTGTCACCGAAAGGTCTCTTATCAAGG TCTATGGACCTTGGAGCGCTCTCGAGCAAGCCGCACGGGTTTGCGAAATGGAGCCGCT TCTTCAAGACATCGTTCACGAGGAAGCCGGCACACTTACACAACCAGTTCAATGGGGA GAAATCACCCCGCAGGCTGGTCTATCTACGGTGCAATCCGCAACAGCGGCTATCCGAG CGTGCGAAAACGGCGAAGTCGATGCCGTCATTGCCTGCCCTCACCATGAAACGGCCAT TCACCGCGCAGGCATAGCGTTCAGCGGCTACCCATCTTTGCTCGCCAATGTTCTTGGCA TGAACGAAGACCAGGTATTCCTGATGCTGGTGGGGGCTGGCCTGCGCATAGTGCATGT CACTTTGCATGAAAGCGTGCGCAGCGCATTGGAGCGGCTCTCTCCTCAGTTGGTGGTCA ACGCGGCGCAGGCTGCCGTGCAGACATGCACCTTACTCGGAGTGCCTAAACCAAAAGT CGCTGTATTCGGGATCAACCCTCATGCATCTGAAGGACAGTTGTTCGGCCTGGAGGACT CCCAGATCACCGTTCCCGCTGTCGAGACACTGCGCAAGCGCGGCCTAGCAGTAGACGG CCCCATGGGAGCTGACATGGTTCTGGCACAGCGCAAGCACGACCTGTATGTAGCCATG CTGCACGATCAGGGCCATATCCCCATCAAGCTGCTGGCACCTAACGGAGCCAGCGCAC TATCTATCGGTGGCAGGGTGGTGCTTTCCAGCGTGGGCCATGGCAGCGCCATGGACAT TGCCGGCCGTGGCGTGGCTGACGCCACGGCCCTCCTACGCACAATAGCCCTACTCGGA GCCCAACCGGTCTGA
aroY	B2DCZ6	ATGCAGAACCCGATCAACGACCTGCGCTCCGCGATCGCGCTGCTGCAACGCCATCCGG GTCACTACATCGAAACCGACCACCCGGTCGACCCGAACGCCGAACTGGCCGGTGTGTA CCGCCACATCGGTGCGGGTGGCACCGTGAAACGTCCGACCCGCACCGGTCCAGCCATG ATGTTCAACAGCGTGAAGGGCTACCCAGGCAGCCGCATCCTGGTGGGCATGCACGCCA GCCGTGAACGTGCCGCCCTGCTGCTGGGCTGCGTGCCAAGCAAACTGGCGCAGCACG TGGGCCAGGCCGTGAAGAACCCGGTGGCCCCAGTGGTGGTGCCAGCCAGCCAAGCCC CATGCCAAGAACAGGTGTTCTACGCCGACGACCCGGACTTCGACCTGCGCAAGCTGCT GCCAGCCCCAACCAACACCCCGATCGATGCCGGTCCGTTCTTCTGCCTGGGCCTGGTG CTGGCGAGCGACCCGGAAGATACCAGCCTGACCGACGTGACCATCCACCGCCTGTGCG TGCAAGAGCGCGACGAGCTGAGCATGTTCCTGGCCGCCGGTCGCCACATCGAGGTGTT CCGCAAGAAGGCCGAAGCCGCCGGTAAGCCGCTGCCGGTGACCATCAACATGGGCCTG GACCCAGCCATCTACATCGGTGCCTGCTTCGAAGCGCCAACCACCCCGTTCGGCTACAA CGAGCTGGGTGTGGCCGGTGCCCTGCGTCAGCAACCGGTGGAACTGGTGCAGGGCGT GGCCGTGAAAGAGAAGGCGATCGCGCGTGCCGAGATCATCATCGAGGGCGAACTGCTG CCAGGCGTGCGCGTGCGCGAAGATCAGCACACCAACACCGGTCACGCCATGCCGGAAT TCCCAGGCTACTGCGGTGAGGCCAACCCGAGCCTGCCGGTGATCAAGGTGAAGGCCGT GACCATGCGCAACCACGCCATCCTGCAGACCCTGGTGGGTCCGGGTGAGGAACACACC ACCCTGGCGGGTCTGCCGACCGAAGCCAGCATCCGCAACGCCGTGGAAGAGGCGATCC CAGGCTTCCTGCAGAACGTGTACGCCCACACCGCCGGTGGCGGTAAGTTCCTGGGCAT CCTGCAGGTCAAGAAGCGCCAGCCGAGCGACGAAGGCCGTCAGGGCCAAGCCGCCCT GATCGCCCTGGCCACCTACAGCGAGCTGAAGAACATCATCCTGGTGGACGAGGACGTG GACATCTTCGACAGCGACGACATCCTGTGGGCCATGACCACCCGCATGCAGGGCGACG

		TGAGCATCACCACCCTGCCAGGCATCCGTGGCCATCAGCTGGACCCGAGCCAGAGCCC AGACTACAGCACCAGCATCCGTGGCAACGGCATCAGCTGCAAGACCATCTTCGACTGC ACCGTGCCGTGGGCCCTGAAAGCCCGTTTCGAGCGTGCCCCATTCATGGAAGTGGACC CGACCCCGTGGGCCCCAGAGCTGTTCAGCGACAAGAAGTAA
Bs2Est	P37967	ATGACTCATCAAATAGTAACGACTCAATACGGCAAAGTAAAAGGCACAACGGAAAACGGC GTACATAAGTGGAAAGGCATCCCCTATGCCAAGCCGCCTGTCGGACAATGGCGTTTTAAA GCACCTGAGCCGCCTGAAGTGTGGGAAGATGTGCTTGATGCCACAGCGTACGGCTCTAT TTGCCCGCAGCCGTCTGATTTGCTGTCACTTTCGTATACTGAGCTGCCCCGCCAGTCCGA GGATTGCTTGTATGTCAATGTATTTGCGCCTGACACCCCAAGTAAAAATCTTCCTGTCATGG TGTGGATTCACGGAGGCGCTTTTTATCTAGGAGCGGGCAGTGAGCCATTGTATGACGGAT CAAAACTTGCGGCACAGGGAGAAGTCATTGTCGTTACATTGAACTATCGGCTGGGGCCGT TTGGCTTTTTGCACTTGTCTTCATTTAATGAGGCGTATTCTGATAACCTTGGGCTTTTAGAC CAAGCCGCCGCGCTGAAATGGGTGCGAGAGAATATTTCAGCGTTTGGCGGTGATCCCGA TAACGTAACAGTATTTGGAGAATCCGCCGGCGGGATGAGCATTGCCGCGCTGCTTGCTAT GCCTGCGGCAAAAGGCCTGTTCCAGAAAGCAATCATGGAAAGCGGCGCTTCTCGAACGA TGACGAAAGAACAAGCGGCGAGCACCTCGGCAGCCTTTTTACAGGTCCTTGGGATTAAC GAGGGCCAACTGGATAAATTGCATACGGTTTCTGCGGAAGATTTGCTAAAAGCGGCTGAT CAGCTTCGGATTGCAGAAAAAGAAAATATCTTTCAGCTGTTCTTCCAGCCCGCCCTTGAT CCGAAAACGCTGCCTGAAGAACCAGAAAAAGCGATCGCAGAAGGGGCTGCTTCCGGTA TTCCGCTATTAATTGGAACAACCCGTGATGAAGGATATTTATTTTTCACCCCGGATTCAGA CGTTCATTCTCAGGAAACGCTTGATGCAGCGCTGGAGTATTTACTAGGGAAGCCGCTGG CAGAGAAAGTTGCCGATTTGTATCCGCGTTCTCTGGAAAGCCAAATTCACATGATGACTG ATTTATTATTTTGGCGCCCTGCCGTCGCCTATGCATCCGCACAGTCTCATTACGCCCCTGT CTGGATGTACAGGTTCGATTGGCACCCGAAGAAGCCGCCGTACAATAAAGCGTTTCACG CATTAGAGCTTCCTTTTGTCTTTGGAAATCTGGACGGATTGGAACGAATGGCAAAAGCGG AGATTACGGATGAGGTGAAACAGCTTTCTCACACGATACAATCAGCGTGGATCACGTTCG CCAAAACAGGAAACCCAAGCACCGAAGCTGTGAATTGGCCTGCGTATCATGAAGAAACG AGAGAGACGCTGATTTTAGACTCAGAGATTACGATCGAAAACGATCCCGAATCTGAAAAA AGGCAGAAGCTATTCCCTTCAAAAGGAGAATAA

Table S3 Primers used in this study.

Primer name	Sequence	Gene source
pKM212-TphAabc-F	GGTACC TTTCACACAGGAAACAGACC ATGAACCACCAGATCCATATCC	*Comamonas sp. strain E6*
pKM212-TphAabc-R	AAGCTT TTATAGCGGCAATGCCATCA	*Comamonas sp. strain E6*
pKE112-TphB-F	GAATTC ATGACAATAGTGCACCGTAG	*Comamonas sp. strain E6*
pKE112-TphB-R	GGTACC TTAGACCGGTTGGGCTCC	*Comamonas sp. strain E6*
pKE112-AroY-F	GGATCC ATGCAGAACCCGATCAACGA	*Enterobacter cloacae*
pKE112-AroY-R	CCTGCAGG TTACTTCTTGTCGCTGAACA	*Enterobacter cloacae*
pET28a-Bs2Est -F	CAT ATGACTCATCAAATAGTAACGAC	*Bacillus subtilis (strain 168)*
pET28a-Bs2Est -R	CTCGAG TTATTCTCCTTTTGAAGGGAATAGC	*Bacillus subtilis (strain 168)*

Table S4 Plasmid and bacterial strains used in this study.

Strains and plasmid	Relevant characteristic	Reference or source
Strains		
E. coli BL21 (DE3)	*E. coli str. B F– ompT gal dcm lon hsdSB(rB–mB–) λ(DE3 [lacI lacUV5-T7p07 ind1 sam7 nin5]) [malB+]K-12(λS)*	
E. coli BS2	*E. coli* BL21(DE3) with pET28a- Bs2Est	In this study
E. coli PCA-1 (TPA to PCA)	*E. coli* BL21(DE3) with pKE112TphB and pKM212 tphAabc	[Kim et al., 2019]
E. coli CTL-1 (TPA to catechol)	*E. coli* BL21(DE3) with pKE112TphBaroY and pKM212 tphAabc	[Kim et al., 2019]
Plasmids		
pET28a-Bs2Est	pET28a; T7 promoter, *pnbA* gene of *Bacillus subtilis (strain 168)*, Km^R	In this study
pKE112TphB	pKE112; P_{tac} promoter, *tphB* gene of *Comamonas sp. (strain E6)*, Amp^R	[Kim et al., 2019]
pKE112TphBaroY	pKE112; P_{tac} promoter, *aroY* gene of *Enterobacter cloacae* inserted into pKE112TphB, Amp^R	[Kim et al., 2019]
pKM212TphAabc	pKM212; P_{tac} promoter, *tphAabc* genes of *Comamonas sp. strain E6*, Km^R	[Kim et al., 2019]

References

[1] C.-G. Park, T.-W. Kim, I.-S. Oh, J. K. Song, D.-M. Kim, *Biotechnol. Prog.* **2009**, *25*, 589-593.

[2] J. F. Sambrook, D. W. Russell, Molecular Cloning: a Laboratory Manual 3rd edn, Cold spring harbor laboratory press, New York, **2001**.

[3] B. Heinze, R. Kourist, L. Fransson, K. Hult, U. T. Bornscheuer, *Protein Eng. Des. Sel.* **2007**, *20*, 125-131

[4] R. Kourist, S. Bartsch, L. Fransson, K. Hult, U. T. Bornscheuer, *ChemBioChem* **2008**, *9*, 67-69.

[5] M. Schmidt, E. Henke, B. Heinze, R. Kourist, A. Hidalgo, U. T. Bornscheuer, *Biotechnology Journal* **2007**, *2*, 249-253.

[6] D. L. (Tyler) Yin, P. Bernhardt, K. L. Morley, Y. Jiang, J. D. Cheeseman, V. Purpero, J. D. Schrag, R. J. Kazlauskas, *Biochemistry* **2010**, *49*, 1931-1942.

[7] R. Roberts, *Polymer* **1969**, *10*, 113-116.

[8] a) E. Barbayianni, C. G. Kokotos, S. Bartsch, C. Drakou, U. T. Bornscheuer, G. Kokotos, *Adv. Synth. Catal.* **2009**, *351*, 2325-2332; b) M. Schmidt, E. Henke, B. Heinze, R. Kourist, A. Hidalgo, U. T. Bornscheuer, *Biotechnol. J.* **2007**, *2*, 249-253.